© 2015. Published by The Company of Biologists Ltd | Development (2015) 142, 1375-1386 doi:10.1242/dev.117093

RESEARCH ARTICLE

TECHNIQUES AND RESOURCES

Activin A directs striatal projection neuron differentiation of human pluripotent stem cells

Charles Arber[1], Sophie V. Precious[2], Serafí Cambray[3], Jessica R. Risner-Janiczek[1], Claire Kelly[2], Zoe Noakes[4], Marija Fjodorova[4], Andreas Heuer[2], Mark A. Ungless[1], Tristan A. Rodríguez[3], Anne E. Rosser[2], Stephen B. Dunnett[2] and Meng Li[1,4,*]

ABSTRACT

The efficient generation of striatal neurons from human embryonic stem cells (hESCs) and induced pluripotent stem cells (hiPSCs) is fundamental for realising their promise in disease modelling, pharmaceutical drug screening and cell therapy for Huntington's disease. GABAergic medium-sized spiny neurons (MSNs) are the principal projection neurons of the striatum and specifically degenerate in the early phase of Huntington's disease. Here we report that activin A induces lateral ganglionic eminence (LGE) characteristics in nascent neural progenitors derived from hESCs and hiPSCs in a sonic hedgehog-independent manner. Correct specification of striatal phenotype was further demonstrated by the induction of the striatal transcription factors CTIP2, GSX2 and FOXP2. Crucially, these human LGE progenitors readily differentiate into postmitotic neurons expressing the striatal projection neuron signature marker DARPP32, both in culture and following transplantation in the adult striatum in a rat model of Huntington's disease. Activin-induced neurons also exhibit appropriate striatal-like electrophysiology *in vitro*. Together, our findings demonstrate a novel route for efficient differentiation of GABAergic striatal MSNs from human pluripotent stem cells.

KEY WORDS: Activin, DARPP32 (PPP1R1B), Lateral ganglionic eminence, Medium spiny neuron, Pluripotent stem cell, Neural differentiation, Huntington's disease, Striatum, Transplantation

INTRODUCTION

The γ-amino butyric acid (GABA) medium-sized spiny neurons (MSNs) are the principal projection neurons of the striatum and are defined by their expression of the dopamine- and cAMP-regulated phosphoprotein (DARPP32; also known as PPP1R1B). It is these cells that specifically degenerate in the early phase of Huntington's disease (HD) (Lange et al., 1976; Reiner et al., 1988; Gerfen, 1992; Ouimet et al., 1984). Unlike some other neurodegenerative diseases, such as Parkinson's disease, which can be effectively managed for years by dopamine-based pharmacotherapy, no effective disease-modifying treatment is currently available for HD. Despite having identified the gene responsible for HD, the precise mechanism of the disease pathology remains to be fully elucidated, although significant progress has been made in recent years, implicating several mechanisms in the process.

Proof of principle has been provided that HD patient-derived human induced pluripotent stem cells (hiPSCs) can serve as a valuable resource to elucidate disease mechanisms in HD and as a platform for drug development (The HD iPSC Consortium, 2012). However, future investigations will require methods that direct human embryonic stem cell (hESC)/hiPSC differentiation efficiently towards a striatal-specific neuronal phenotype to understand aspects of the disease such as the specific neurotoxicity of the mutant huntingtin (HTT) protein to MSNs. Moreover, intrastriatal transplantation of human fetus-derived ganglionic eminence (GE) cells has shown some functional benefit for HD patients (Rosser and Bachoud-Lévi, 2012). Hence, MSNs derived from hiPSCs and/or hESCs promise hope for developing cell-based therapy for HD.

The striatal MSNs are derived from the dorsal domain of the ventral telencephalon in the region termed the lateral ganglionic eminence (LGE) (Olsson et al., 1998), which lies ventral to the developing cortex and dorsolateral to the medial ganglionic eminence (MGE). The progenitor zone of the LGE gives rise to striatal projection neurons (the MSNs) and olfactory bulb interneurons, whereas the progenitor zone of the MGE produces cortical and striatal interneurons (Campbell, 2003; Marín and Rubenstein, 2003). The cellular identity of LGE progenitors can be defined by the combinatorial expression of several transcription factors, including Gsx2, Dlx2, Ctip2, Nolz1, FoxP1 and FoxP2 (Arlotta et al., 2008; Takahashi et al., 2003; Chang et al., 2004; Urbán et al., 2010). These molecules also serve as important intrinsic regulators controlling the fate specification of MSNs.

Molecular signalling is essential for the tightly regulated patterning of transcription factors that encode distinct neuronal subtypes during neural development. In the forebrain, temporally and spatially regulated expression of the signalling molecules sonic hedgehog (Shh) and members of the Wnt, FGF and TGFβ protein families act in concert to control dorsoventral and rostrocaudal fate specification (Harrison-Uy and Pleasure, 2012; Manning et al., 2006). For instance, Shh induces and maintains expression of the homeobox gene *Nkx2.1* in the MGE (Gulacsi and Anderson, 2006), while β-catenin-mediated Wnt signals are required to maintain the dorsal telencephalic markers Emx1, Emx2 and Ngn2 (Backman et al., 2005). By contrast, activation of the canonical Wnt signalling pathway in the subpallium leads to repression of ventral telencephalic determinants including Nkx2.1, Gsx2, Dlx2 and Mash1. By applying this developmental knowledge, researchers have employed a defined dose of Shh, or Shh together with pharmacological inhibition of Wnt signalling, to obtain LGE-like neural progenitors from hESCs (Aubry et al., 2008; Li et al., 2009; Ma et al., 2012; Carri et al., 2013). However, genetic perturbation of the Shh-Gli pathway at the time of subpallial patterning in mouse

[1]Medical Research Council Clinical Sciences Centre, Imperial College London, Hammersmith Hospital Campus, Du Cane Road, London W12 ONN, UK. [2]Brain Repair Group, Neuroscience and Mental Health Research Institute, School of Bioscience, Cardiff University, Cardiff CF10 3AX, UK. [3]National Heart and Lung Institute, Imperial College London, Hammersmith Hospital Campus, Du Cane Road, London W12 ONN, UK. [4]Stem Cell Neurogenesis Group, Neuroscience and Mental Health Research Institute, School of Medicine and School of Bioscience, Cardiff University, Cardiff CF24 4HQ, UK.

*Author for correspondence (lim26@cf.ac.uk)

Received 28 August 2014; Accepted 6 February 2015

Development (2015) 142, 1375-1386 doi:10.1242/dev.117093

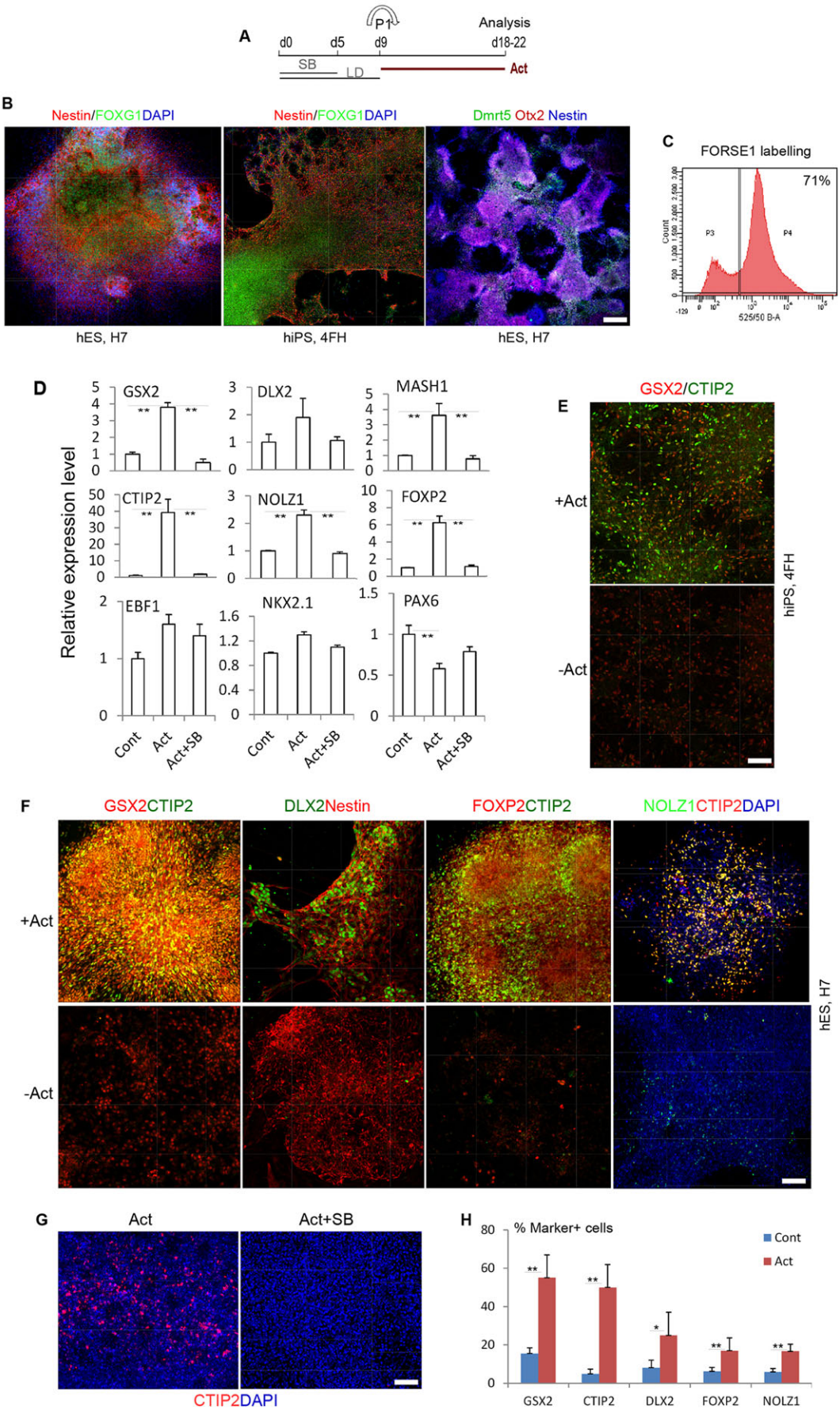

Fig. 1. See next page for legend.

Development (2015) 142, 1375-1386 doi:10.1242/dev.117093

Fig. 1. Activin induces LGE progenitor characteristics and striatal differentiation of hPSCs. (A) Experimental scheme. hESC or hiPSC monolayer cultures were exposed to activin from day 9 to day 18 or 22, when the cultures were harvested for analysis. SB, SB431542; LD, LDN and dorsomorphin; Act, activin A. (B) Antibody staining of a day 18 control culture for the pan-neuroepithelial marker nestin and telencephalic-specific markers FOXG1, OTX2 and cortical neuroepithelial marker DMRT5. Nuclei are counterstained with DAPI (blue). (C) Flow cytometry histogram showing that 71% of the total cell population were FORSE1$^+$ forebrain neural progenitors. (D) qPCR analysis of LGE/striatal and other forebrain regional markers of day 18 cultures following activin treatment from day 9 with or without the Smad inhibitor SB431543, compared with no-activin controls (Cont; set as 1). Data shown are the average of two independent sets of experiments each with duplicate cultures. $^{**}P\leq0.01$, one-way ANOVA followed by Duncan's post-hoc test. (E) Day 18 cultures of 4FH hiPSCs immunostained for GSX2 and CTIP2. (F) Day 22 cultures of H7 hESCs exposed to activin from day 9 and immunostained as indicated. (G) CTIP2 staining of day 20 cultures of H7 cells treated with activin from day 9 in the presence or absence of SB431543 from day 10. (H) Quantification of immunostaining of H7 cells in F. $^{*}P\leq0.05$, $^{**}P\leq0.01$, Student's *t*-test between control and activin-treated samples for each marker. Scale bars: 100 µm in B; 75 µm in E,F; 60 µm in G.

models does not affect LGE induction and subsequent striatal MSN neurogenesis (Rallu et al., 2002; Xu et al., 2010; Machold et al., 2003). It is therefore likely that the DARPP32$^+$ neurons generated in Shh-treated cultures occur via an indirect signalling cascade of MGE fate induction, rather than by direct instruction of LGE fate.

Activin A (referred to hereafter as activin) is a multifunctional TGFβ family protein that has been shown to induce forebrain neurogenesis in a neuronal subtype-restricted manner (Sekiguchi et al., 2009; Abdipranoto-Cowley et al., 2009). Both activin receptors and the activated (phosphorylated) activin effector protein Smad2 are expressed in the developing LGE that later forms the striatum (Maira et al., 2010; Feijen et al., 1994), implicating a role for activin and/or TGFβ family proteins in striatal neuron differentiation. Using hESCs and hiPSCs as a model, we show that activin induces LGE characteristics in hESC/hiPSC-derived anterior neural progenitors. These LGE progenitors readily give rise to functional GABAergic neurons expressing DARPP32 in culture and are engraftable in a rodent model of HD (Ouimet et al., 1984). Therefore, our study identifies activin as a molecule capable of specifying lateral forebrain identity, producing a significant population of mature DARPP32$^+$ neurons from both hESC and hiPSC cultures. Furthermore, this novel protocol would provide a valuable tool for modelling HD, pharmacological trials and cell-based therapy for HD.

RESULTS

Activin induces an LGE-like progenitor fate

We have shown previously that activin can induce a caudal ganglionic eminence (CGE)-like fate from human and mouse pluripotent stem cell (PSC)-derived forebrain neural progenitors, leading to the production of calretinin (CR; calbindin 2)$^+$ cortical interneurons (Cambray et al., 2012). The CGE shares a range of important molecular characteristics with the LGE and has been described as a caudal extension of the LGE (Flames et al., 2007). Similar to neural induction in the developing embryo, PSC neural development follows an anterior first, posterior later temporal axis. We therefore postulated that a modification of the CGE induction protocol, by shifting the activin exposure time window forward and using an optimal dosage, would capture the most rostral telencephalic neural progenitors disposed to LGE specification.

Forebrain neural progenitors were generated using a simplified monolayer-based differentiation scheme that replaces KSR with N2B27 during neural induction and in the presence of BMP/Smad inhibitors LDN, dorsomorphin (referred to together as LD) and SB431542 (Fig. 1A) (Cambray et al., 2012). Under this condition, hESCs (H7, H1 and H9) and hiPSCs (2F8, 4FH) rapidly downregulated the expression of the pluripotent genes *OCT4* (*POU5F1*) and *NANOG* and acquired neuroepithelial progenitor characteristics by day (d) 9-10 of monolayer differentiation (MD) (Cambray et al., 2012). The forebrain neural progenitor identity was verified by expression of the forkhead transcription factor FOXG1, OTX2 and cell surface marker FORSE1 epitope (Fig. 1B,C) (Xuan et al., 1995; Elkabetz et al., 2008). In the absence of exogenous factors, these forebrain progenitors comprise a mix of dorsal and ventral entities, as demonstrated by the co-existence of cells expressing cortical (DMRT5; also known as DMRTA2) and ventral forebrain (GSX2) transcription factors (Fig. 1B,E,F) (Gennet et al., 2011).

The LGE and its ventral neighbour the MGE can be distinguished by the differential combinatorial expression of transcription factors. Although both regions express GSX2, DLX2 and MASH1 (ASCL1), striatal neuron precursors in the LGE are characterised by their differential expression of CTIP2 (BCL11B), FOXP1, FOXP2, EBF1 and NOLZ1 (ZFP503), whereas cells of the MGE express NKX2.1 and LHX6/8 but not the above striatal genes (Arlotta et al., 2008; Takahashi et al., 2003; Chang et al., 2004; Urbán et al., 2010; Garel et al., 1999). After a pilot assay that tested a range of activin doses (5-50 ng/ml) on selected striatal marker gene expression, we performed all subsequent experiments using 25 ng/ml activin.

Following a 9-day exposure to activin from day 9 (Fig. 1A), we detected a pronounced increase of *CTIP2* transcript (40-fold; Fig. 1D). Increased RNA level was also detected for all other LGE/striatum-expressed transcription factors analysed (*FOXP2*, 7-fold; *DLX2*, 5-fold; *GSX2*, 3.8-fold; *MASH1*, 3.5-fold; *NOLZ1*, 2.3-fold; and *EBF1*, 1.5-fold). However, addition of a specific activin/Smad inhibitor, SB431543, completely blocked the regulation of these LGE/striatal transcripts by activin (Fig. 1D), suggesting that the induction of the LGE/striatal characteristics requires SMAD2/3 pathway activation in this system. Furthermore, activin treatment resulted in a reduction of *PAX6* transcripts, suggesting suppression of dorsal telencephalic characteristics, whereas no significant change was observed for the MGE transcripts *NKX2.1* and *EBF1* (Fig. 1D). These data suggest that activin preferentially induces LGE/striatal characteristics in neurally induced hiPSCs.

To further demonstrate a preferential induction of LGE/striatal cellular phenotype by activin, we performed immunostaining for GSX2, DLX2, CTIP2 and FOXP2 (Fig. 1E,F; supplementary material Fig. S1). We consistently observed an increase in the number of GSX2$^+$ cells in activin-treated cultures compared with controls. In the control cultures, few cells were immunoreactive to CTIP2, NOLZ1, FOXP2 or DLX2 (all <4%; Fig. 1E,F). By contrast, abundant CTIP2$^+$ (50±12%), DLX2$^+$ (25±12%), GSX2$^+$ (55±10%), FOXP2$^+$ (16±6.7%) and NOLZ1$^+$ (16.7±1.7%) cells were found in activin-treated cultures (Fig. 1E,F,H). Moreover, addition of SB431542 suppressed the generation of CTIP2$^+$ cells by activin (Fig. 1G). The effect of activin can be readily replicated in independent hESC (H7) and hiPSC (4FH) lines (Fig. 1E,F).

Activin could increase the number of striatal precursor cells by two possible mechanisms: by directly conferring a striatal phenotype on forebrain progenitors or by selectively promoting the proliferation of pre-patterned striatal progenitors. To distinguish between these possibilities, we performed an EdU-incorporation study on day 16 cultures treated with or without activin for 6 days.

Development (2015) 142, 1375-1386 doi:10.1242/dev.117093

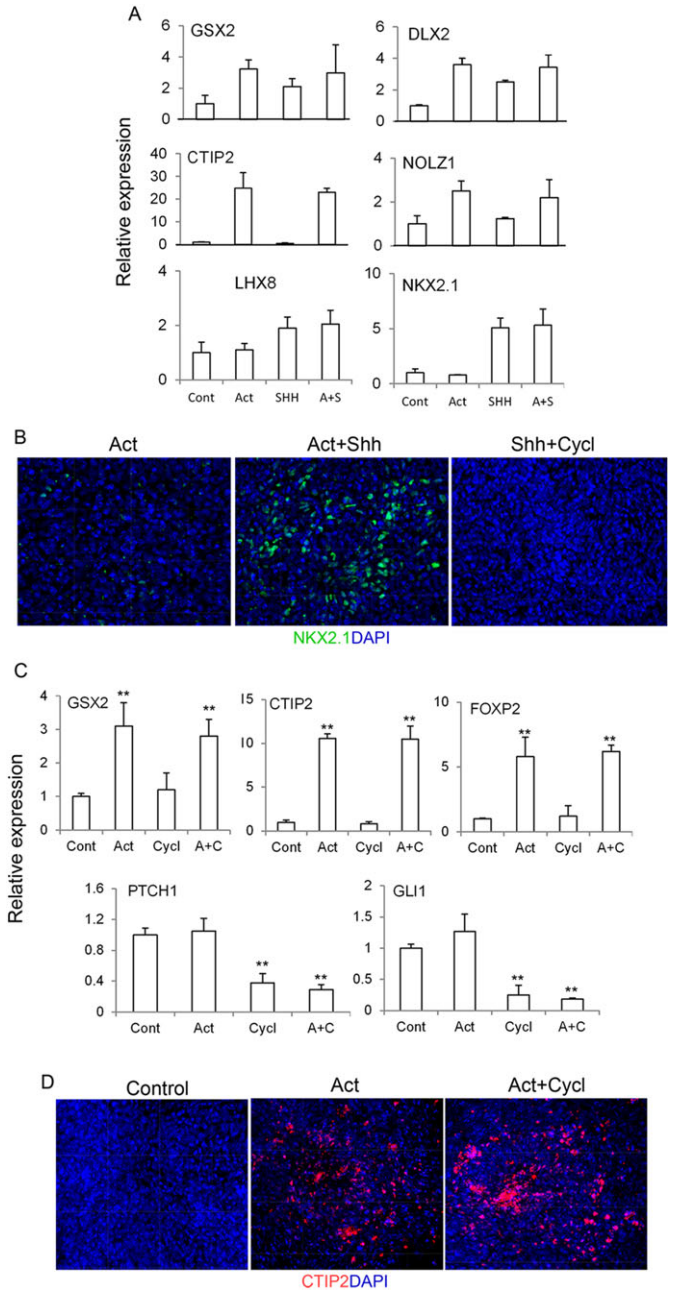

Fig. 2. Activin induction of LGE characteristics does not require Shh signalling. (A) Day 9 cultures were treated with activin, Shh or both. Cultures were harvested 4 days later for qPCR. (B) NKX2.1 staining of day 20 cultures treated with activin alone (left), activin plus 100 ng/ml Shh, or 100 ng/ml Shh plus 2 µM cyclopamine (Cycl) from day 9. (C) Day 9 cultures were treated with activin, cyclopamine or both. Cultures were harvested 4 days later for qPCR. $^{**}P \leq 0.01$, one-way ANOVA. (A,C) Untreated control (Cont) was set to 1. (D) CTIP2 staining of day 20 control culture and cultures treated with activin in the presence or absence of cyclopamine from day 9.

Cultures were exposed to the nucleotide analogue EdU for 1 h before being processed for chemical-based EdU staining. Consistent with our previous finding that activin has a pro-differentiation effect on forebrain neural progenitors, we found that activin treatment resulted in a reduction in the number of EdU^+ cells (supplementary material Fig. S2). Furthermore, the degree of reduction in EdU^+ cells in the $GSX2^+$ ventral progenitor group is similar to that for the total cell population, indicating that activin did not preferentially affect the mitotic profile of the $GSX2^+$ subpopulation. Our data therefore suggest that activin patterns the forebrain progenitors to acquire an LGE/striatal fate.

Differential activity of activin and Shh in regulating ventral forebrain characteristics

Shh is a secreted signalling molecule with a crucial role in the generation of ventral cell types along the entire rostrocaudal axis of the neural tube. Shh was first applied in an hESC differentiation protocol for generating $DARPP32^+$ neurons (Aubry et al., 2008) and again recently with or without combinatorial inhibition of Wnt signalling (Ma et al., 2012; Carri et al., 2013; Nicoleau et al., 2013). The effect of Shh on the generation of ventral forebrain cellular phenotypes might be due to the derepression of GLI3, which is a key factor that dorsalises hESC-derived neural progenitors (Li et al., 2009). However, the above-mentioned ESC studies do not necessarily suggest a direct role for Shh in LGE/striatal fate specification. Furthermore, genetic study of *Gli3* hypomorphic mutant mice, which exhibit elevated Shh signalling in the ventral forebrain, revealed aberrant patterning of the LGE exemplified by ectopic expression of MGE characteristics (Magnani et al., 2010); this study suggests that the primary target of Gli3 suppression is the MGE.

We investigated the ability of Shh to induce LGE/striatal characteristics and compared the effect with that of activin. We observed a dose-dependent increase of MGE-specific *NKX2.1* transcripts in response to Shh (Zhao et al., 2003), and a small increase in *GSX2* and *DLX2*, which are expressed in both the MGE and LGE (supplementary material Fig. S3A). *LHX8*, a transcription factor expressed specifically in immature MGE-derived interneurons, is also upregulated in response to Shh. However, transcripts preferentially expressed in the LGE, such as *NOLZ1*, *FOXP2* and *CTIP2*, showed little or no graded response (supplementary material Fig. S3A). This is in stark contrast to the effect of activin on these cells, which induced a dose-dependent increase in LGE and pan-GE transcripts, such as *GSX2*, *DLX2*, *CTIP2* and *FOXP2*, with little impact on *NKX2.1* (Fig. 1D; data not shown). These data are consistent with the findings obtained from mouse genetics studies and support the view that, although the MGE inductive property can be attributed to Shh, Shh does not have a specific role in LGE specification of hESC-derived forebrain progenitors.

We then investigated whether Shh could potentiate activin-mediated LGE induction. We cultured d10 forebrain progenitors with activin, with and without increasing concentrations of Shh, and examined the expression of the pan-GE, LGE and MGE markers by qPCR 3 days later. Again, Shh treatment led to an upregulation of MGE marker genes *NKX2.1* and *LHX8* (Fig. 2A). However, the addition of Shh did not increase the transcript level of LGE and pan-GE markers (*GSX2*, *DLX2*, *CTIP2* and *NOLZ1*) above the level achieved by activin alone (Fig. 2A; supplementary material Fig. S3B). Immunostaining revealed a robust induction of $NKX2.1^+$ cells in response to Shh (Fig. 2B). These observations indicate that Shh does not enhance the activity of activin in the induction of LGE characteristics.

We then examined whether activin-induced LGE gene expression requires Shh signalling by blocking it with the naturally occurring Shh antagonist cyclopamine. At a concentration that blocks Shh-induced NKX2.1 induction (Fig. 2B), cyclopamine alone did not affect *CTIP2* or *FOXP2* expression (Fig. 2C). Moreover, cyclopamine did not affect activin-mediated upregulation of the LGE-enriched genes or the number of $CTIP2^+$ cells induced by activin (Fig. 2D). Together, our data indicate that activin induces LGE/striatal progenitor fate independently of Shh signalling.

Development (2015) 142, 1375-1386 doi:10.1242/dev.117093

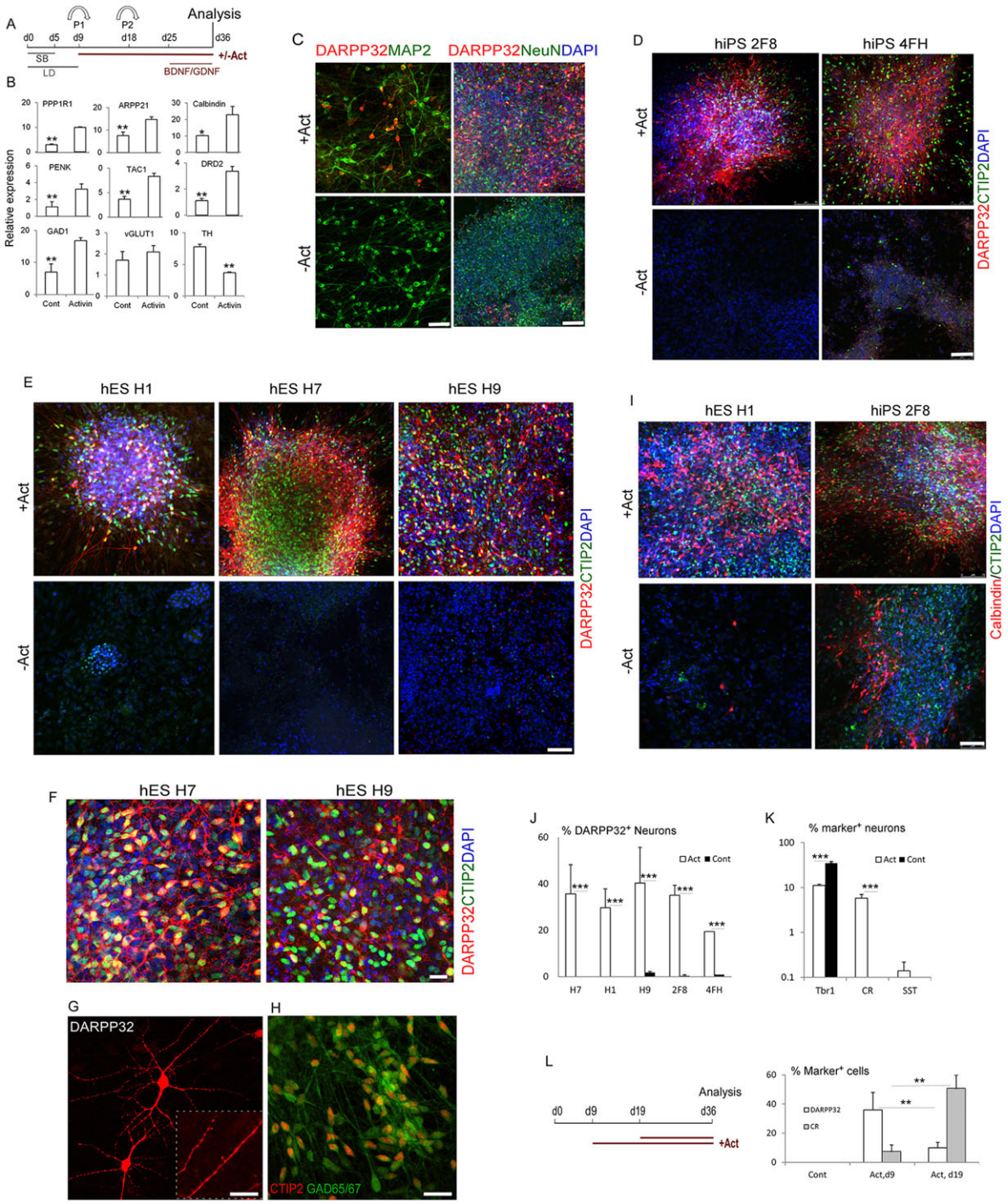

Fig. 3. Efficient generation of striatal projection neurons by activin stimulation. (A) Experimental scheme. (B) qPCR analysis for striatal projection neuron-expressed genes and neuronal transmitter genes. *$P \leq 0.05$, **$P \leq 0.01$, Student's *t*-test. (C-I) Immunostaining of day 36-40 cultures for the indicated markers. (G) DARPP32 with a high-magnification inset showing dendrites. (J) Quantification of immunostaining in D,E, showing the percentage of DARPP32$^+$ neurons. (K) Quantification of other neuronal subtypes. ***$P \leq 0.001$, Student's *t*-test between control and activin-treated groups for hPSC lines in J and TBR1 and CR in K. (L) Minimal requirement for activin as evaluated by DARPP32$^+$ neuron production. **$P \leq 0.01$, two-way ANOVA. Scale bars: 25 µm in G; 40 µm in C left, F,H; 75 µm in C right, D,E,I.

Efficient generation of DARPP32$^+$ GABAergic neurons from activin-patterned neural precursors

To investigate whether the observed induction of striatal precursor characteristics translates to MSN production, we assessed a panel of subtype-specific late neuronal markers by qPCR and immunocytochemistry on day 36 cultures under the scheme outlined in Fig. 3A. qRT-PCR analysis revealed an increase in the transcript levels of several striatal MSN gene markers in activin-treated cultures compared with untreated controls (Fig. 3B). DARPP32 is the most commonly used definitive marker for mature MSNs. We observed a 5-fold increase in the transcript level of *DARPP32* (*PPP1R1B*) in cultures exposed to

Development (2015) 142, 1375-1386 doi:10.1242/dev.117093

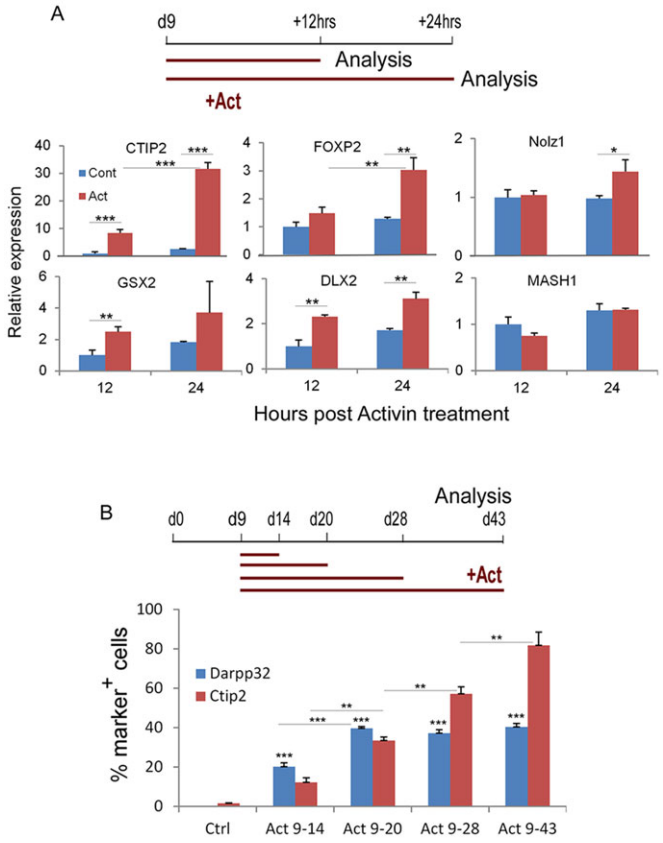

Fig. 4. Rapid induction and maintenance of CTIP2 by activin. (A) qPCR analysis of LGE/striatal marker genes of day 9 cultures exposed to 12 or 24 h activin treatment, as compared with no-activin controls (12 h value set as 1). Data shown are the average of triplicate cultures from one set of experiments. (B) H9-derived forebrain progenitors were treated with activin from day 9 to day 14, 20, 28 or 43. Cells were fixed at day 43 and immunostained for DARPP32 and CTIP2. $P \leq 0.05$, $^{**}P \leq 0.01$, $^{***}P \leq 0.001$, two-way ANOVA followed by Bonferroni correction for multiple comparisons.

activin compared with untreated controls. *ARPP21* (cAMP-regulated phosphoprotein) and the calcium-binding protein calbindin (calbindin 1) are two further genes with enriched expression in the striatum. The RNA levels of both markers increased in activin-treated cultures. Additionally, we examined proenkephalin (*PENK*) and tachykinin 1 (*TAC1*; substance P). (Nikoletopoulou et al., 2007; Chen et al., 2009). The differential expression of these two peptides and dopamine D1 and D2 receptors (DRD1 and DRD2) divide the striatal neurons into two distinct groups with different connectivity (Uhl et al., 1988). MSNs constituting the direct pathway express DRD1 and substance P, and project primarily to the pars reticulata of the substantia nigra. MSNs of the indirect pathway express DRD2 and enkephalin and send their primary projections to the globus pallidus. All these marker genes are upregulated in activin-treated cultures (Fig. 3B; data not shown). Moreover, activin stimulation resulted in an increase in the levels of *GAD1*, which encodes one of several forms of glutamic acid decarboxylase, an enzyme responsible for catalysing the production of GABA. By contrast, no change was observed for the glutamatergic neuron transcript vesicular glutamate transporter 1 (*VGLUT1*; also known as *SLC17A7*). It is noteworthy that the dopamine neuron associated transcript, tyrosine hydroxylase (*TH*), was significantly decreased in activin cultures (Fig. 3B).

Immunocytochemical staining of activin-treated cultures supports the above transcript analysis (Fig. 3C-L). Cells positively stained for DARPP32 were common in the culture wells (Fig. 3C-E). All DARPP32$^+$ neurons expressed the neuronal markers MAP2 and NeuN (RBFOX3) (Fig. 3C), demonstrating their neuronal identity. High-magnification images revealed that the DARPP32$^+$ cells exhibit a branching, multipolar morphology, with numerous spines in neuronal processes (Fig. 3F,G); double immunostaining for DARPP32 and the post-synaptic density marker PSD95 (DLG4) showed abundant PSD95 along the neuronal processes, hinting at functionality of the cells (supplementary material Fig. S4). By contrast, DARPP32 staining was almost completely absent from control cultures. The striatal identity of these cells was further validated by co-expression of a second MSN marker, CTIP2, in all DARPP32$^+$ cells (Fig. 3D-F). Although not restricted to the striatum, calbindin is expressed by MSNs outside the striatal patches. We found that a proportion of the CTIP2$^+$ cells co-express calbindin and that all CTIP2$^+$ cells stained positively for GAD65/67 (*GAD2/1*) (Fig. 3H,I). Thus, the molecular characteristics of activin-induced DARPP32$^+$ cells fit the essential profile of GABAergic striatal projection neurons.

Importantly, the inductive activity of activin on DARPP32$^+$ neurons was observed in all five PSC lines tested (H1, H7 and H9 hESCs, 2F8 and 4FH hiPSCs) and independent experimental settings. In all cases, there were fewer than 1% DARPP32$^+$ cells in basal culture conditions, whereas 20-50% DARPP32$^+$ neurons were obtained in activin-treated cultures depending on the PSC lines (Fig. 3J). In addition to DARPP32$^+$ cells, 6±1.2% CR$^+$ neurons were found in cultures exposed to activin from d9 (Fig. 3K). However, the production of DARPP32$^+$ cells reduced to only 10% when activin was added from d19, in contrast to 50.8±9.1% CR$^+$ neurons under the same conditions (Fig. 3L) (Cambray et al., 2012). Moreover, we found a small proportion of TBR1$^+$ cells and even smaller numbers of somatostatin (SST)$^+$ neurons in activin-treated cultures (Fig. 3K). We did not detect parvalbumin$^+$ interneurons and dopaminergic cells in either the control or activin-treated cultures.

Together, our data demonstrate that activin primes an LGE/striatal regional fate during neuralisation of hPSCs, which leads to the efficient generation of GABAergic neurons with MSN characteristics.

Rapid induction and maintenance of CTIP2 by activin

To begin to elucidate how activin-induced LGE/striatal fate may be mediated, we performed 12 h and 24 h short-term activin treatment on d9 forebrain progenitors and examined the regulation of LGE/striatal regulator gene markers by qPCR (Fig. 4A). An increase of *CTIP2* (8-fold), *GSX2* (2.5-fold) and *DLX2* (2.3-fold) was already evident at 12 h post-stimulation. Interestingly, the *CTIP2* transcript level increased further at 24 h, leading to a greater difference (12-fold) between activin-treated and untreated control cultures. In addition, *FOXP2* and *NOLZ1* transcript levels were moderately increased (2.4-fold and 1.4-fold, respectively) 24 h after activin treatment, whereas no change was observed for *MASH1* at either 12 or 24 h. These temporal gene expression analyses point to a potential direct regulatory activity of activin on *CTIP2*, a transcription factor known to be required for striatal projection neuron development (Arlotta et al., 2008).

The rapid induction of *CTIP2* by activin raised the question of whether a continuous activin treatment from d9 is necessary for the generation of DARPP32$^+$ neurons. We therefore exposed d9 hESC-derived forebrain progenitors to 5, 11, 19 and 34 days of activin treatment. We found that all activin-treated cultures generated

Development (2015) 142, 1375-1386 doi:10.1242/dev.117093

DARPP32$^+$ neurons, compared with none under the control condition. Cultures with 11 days (day 9-20) of exposure to activin produced a similar number of DARPP32$^+$ neurons as those with longer (d9-28 and d9-43) activin treatment. However, cultures with 5 days of activin exposure produced only half the number of DARPP32$^+$ cells (Fig. 4B). Thus, activin treatment from d9-20 is sufficient for the production of DARPP32$^+$ cells. Intriguingly, we observed a steady increase in the number of CTIP2$^+$ neurons with increasing activin treatment time, suggesting that activin signalling might be required for the stable maintenance of a CTIP2$^+$ phenotype.

Electrophysiological characterisation of activin-treated neurons

To examine the functional properties of these neurons, we conducted whole-cell electrophysiological recordings on cultures aged between d35 and d93 (n=60; Fig. 5A). During recording, we filled some of the neurons with Alexa Fluor hydrazide (AF488h) for the purposes of post-hoc immunolabelling and morphological analysis (n=21; Fig. 5B). After recording, the cells were fixed and stained for GAD65/67 and DARPP32 (Fig. 5C-F). Of the 21 neurons that were successfully filled and recovered for immunolabelling, 16 (76%) were GAD67$^+$, whereas 13 (62%) were DARPP32$^+$ (it is likely that, in some of these cases, GAD67 and/or DARPP32 was washed out as a result of the whole-cell recording configuration). All 13 DARPP32$^+$ neurons co-expressed GAD65/67. Alexa Fluor labelling helped to visualise the spiny morphology, which cannot be seen via DARPP32 immunocytochemistry (Fig. 5G).

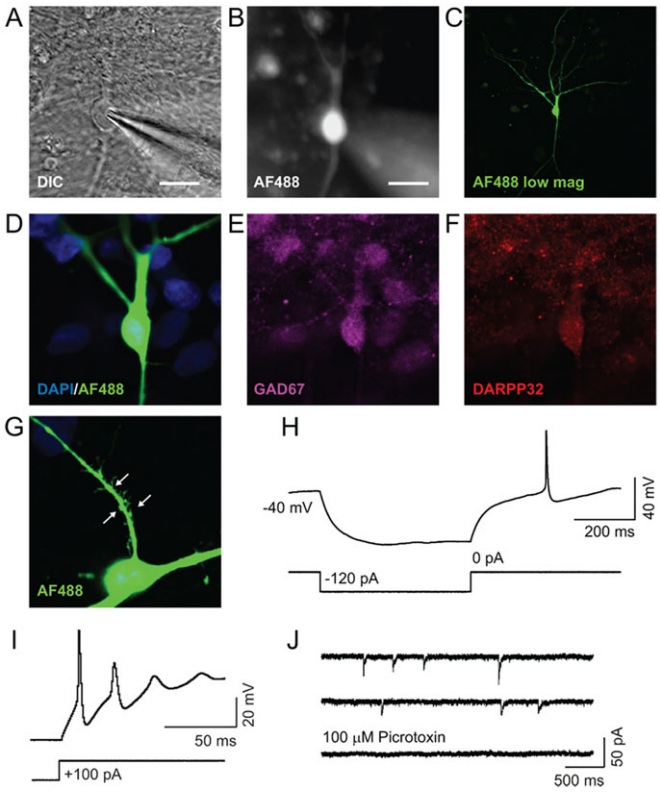

Fig. 5. Electrophysiological properties of activin-induced GABAergic neurons. (A,B) Differential interference contrast (DIC) image from a whole-cell recording of a differentiated neuron that has been filled with AF488 hydrazide (B). Scale bars: 20 µm. (C) Confocal image of a neuron filled with AF88 hydrazide during recording, and fixed post-recording. (D-F) Confocal images confirming that the recorded neurons (green, D) express the GABAergic markers GAD67 (E) and DARPP32 (F). (G) Magnified view of AF488-filled neuronal spines. Arrows indicate the spiny morphology. (H) Delayed action potential generation was observed after repolarisation from a hyperpolarised state. (I) Evoked action potentials generated in response to a depolarising 100 pA current injection. (J) mIPSCs were observed in the presence of 1 µM tetrodotoxin in the external solution and high [Cl$^-$] in the recording pipette. mIPSCs were blocked with 100 µM picrotoxin, confirming their GABAergic identity.

First, we recorded the passive membrane properties of the neurons during differentiation (supplementary material Table S1). All cells exhibited a negative resting membrane potential (−44±1.7 mV, n=41). In addition, capacitance (23.7±1.54, n=58), series resistance (16±0.79 MΩ, n=58) and input resistance (760±123 MΩ, n=60) values all remained constant during maturation in culture (d35-93). We next examined the firing properties of the differentiated neurons. Interestingly, in response to the offset of a hyperpolarising current pulse, the neurons exhibited a delay in action potential firing (Fig. 4H). This latency to fire is characteristic of MSNs (Nisenbaum et al., 1994; Klapstein et al., 2001). Moreover, all neurons fired action potentials in response to a depolarising stimulus (n=42; Fig. 5I).

Finally, we investigated whether these neurons form functional GABAergic synapses. We conducted recordings with chloride-loaded pipettes, which allowed us to resolve large GABAergic events as inward currents at −70 mV (see Materials and Methods). Miniature inhibitory postsynaptic currents (mIPSCs) were consistently observed in these neurons (n=7; Fig. 5J). These events displayed an amplitude of 23.7±1.81 pA (n=7) and occurred with a frequency of 0.11±0.02 Hz (n=7). In all observed cases, mIPSCs were completely blocked upon application of the $GABA_A$ receptor antagonist picrotoxin (100 µM, n=4/4; Fig. 5J).

Taken together, these data demonstrate that activin promotes the efficient generation of functional GABAergic neurons within this culture system.

Robust differentiation and survival of hESC-derived DARPP32$^+$ neurons following transplantation in a rat model of HD

Cellular transplantation is a valuable tool for stringent evaluation of the fate commitment of PSC-derived neuronal phenotypes. We explored the capacity of activin-induced LGE-like progenitors for striatal neuron differentiation and integration in the brains of a rat model of HD. Activin-induced progenitors from H7 hESCs were disassociated into single-cell suspensions at d20 of *in vitro* differentiation and transplanted unilaterally into quinolinic acid-lesioned adult rat striatum (Fig. 6A). Apomorphine-induced rotations showed no overall improvement of the transplanted rats over the 16-week post-transplantation period (supplementary material Fig. S5). Groups of rats were sacrificed 4, 8 and 16 weeks after the engraftment of cells, and the grafted cells were identified by immunohistochemistry using an antibody specific for human nuclei (HuNu) (Fig. 6B).

At 4 weeks post-transplantation, the majority of HuNu$^+$ transplanted cells were nestin$^+$, indicating an immature neural phenotype (Fig. 6C). However, nestin immunoreactivity within the graft was low at 8 weeks post-transplantation, and absent after 16 weeks. Reinforcing this finding, Ki67$^+$ proliferative cells were present within the grafts at 4 weeks post-transplantation, rare in 8-week grafts and absent from 16-week grafts (with the exception of low-level host cell proliferation, which might hint at a non-neuronal response to the graft procedure) (Fig. 6D). DARPP32$^+$ cells were first detected in 8-week-old grafts, although in low numbers (Fig. 6E). However, at 16 weeks post-transplantation a significant proportion of graft-derived

Development (2015) 142, 1375-1386 doi:10.1242/dev.117093

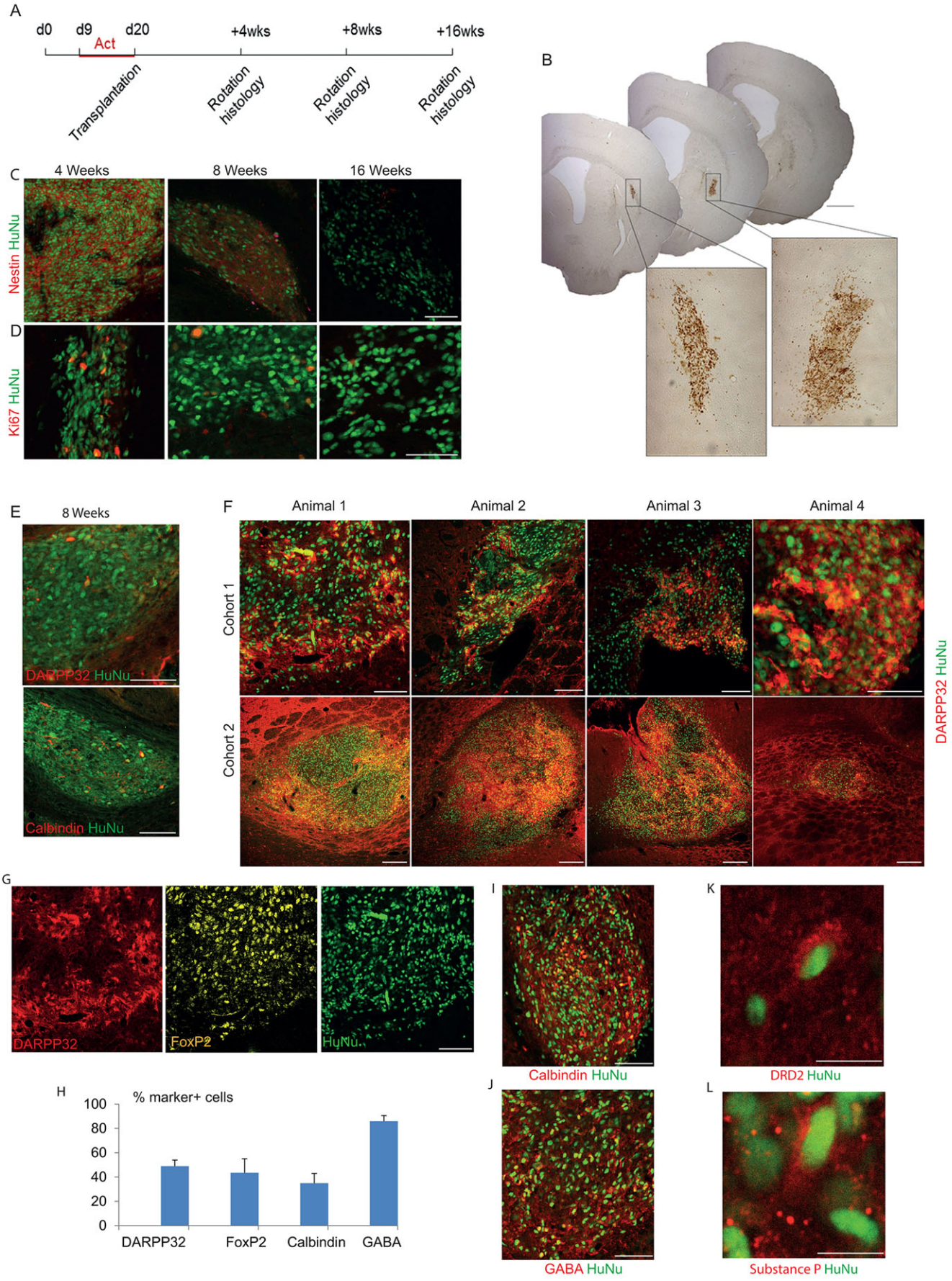

Fig. 6. See next page for legend.

Development (2015) 142, 1375-1386 doi:10.1242/dev.117093

Fig. 6. Robust survival and striatal neuronal differentiation of activin-induced neural progenitors in the adult rat brain. (A) Experimental scheme. (B) Representative low-magnification images of brain sections analysed by HuNu immunohistochemistry at 8 weeks post-transplantation, revealing relatively small grafts with no evidence of overgrowth. Bottom panels are higher magnification photomicrographs of the grafts. (C,D) Microtome sections of brains at 4, 8 and 16 weeks post-transplantation were analysed by immunohistochemistry for HuNu and nestin or Ki67. (E) Immunostaining of 8-week-old grafts for HuNu and DARPP32 or calbindin. (F) DARPP32 and HuNu double staining of 16-week-old grafts. (G) Triple staining for DARPP32, FOXP2 and HuNu on a section of a 16-week-old graft. (H) Quantification of immunostaining of striatal markers, shown as a percentage of $HuNu^+$ cells. (I-L) Immunostaining of 16-week-old grafts for the indicated markers. Unless specified otherwise, images are from 16-week-old grafts. Scale bars: 1 mm in B (low magnification); 100 µm in C-G,I,J; 10 µm in K,L.

cells exhibited high levels of DARPP32 immunostaining, constituting 49±5% of $HuNu^+$ graft cells (Fig. 6F,H). $HuNu^+$ cells were found in 11 of 13 recipient rats analysed at 16 weeks, and all these 11 grafts contained $DARPP32^+$ cells (Fig. 6F; data not shown). FoxP2 and calbindin are two further markers expressed by a subset of striatal projection neurons. We found that 43±11% and 35±8% of $HuNu^+$ cells co-expressed FoxP2 and calbindin, respectively, in 16-week grafts (Fig. 6G-I). The vast majority of grafted cells were $GABA^+$ (86 ±4.6%; Fig. 6H,J). We could find both substance P^+ and $DRD2^+$ cells, suggesting that both the direct and indirect subtypes of MSNs were present within the graft (Fig. 6K,L).

We did not detect any $HuNu^+$ cells co-stained for TH (supplementary material Fig. S6A). However, there were abundant TH^+ fibres surrounding $HuNu^+$ cells, suggesting that the grafts are innervated by the host dopaminergic neurons. Similarly, $VGLUT1^+$ puncta were also abundant in the graft core (supplementary material Fig. S6B). In order to detect potential neuronal process outgrowth to the host brain, we performed immunostaining for human-specific neural cell adhesion molecule (hNCAM; also known as NCAM1), which labels neuronal membrane. hNCAM and HuNu staining overlap in corresponding adjacent sections in the host striatum (supplementary material Fig. S6C). However, more posterior in the globus pallidus (supplementary material Fig. S6D) and in the midbrain (supplementary material Fig. S6E), where HuNu staining is absent and 2400-2920 µm away from the HuNu, small tracts of $hNCAM^+$ fibres were detected. Future pathway-tracing studies will identify the extent to which these projections actually regrow following stem cell-derived grafting, as has been previously observed following embryonic striatal grafting (Nisenbaum et al., 1994; Klapstein et al., 2001).

Overgrowth of grafted cells, either as neural or teratoma-like tissue, appears to be a common feature in previous reports of hPSC-derived striatal GABAergic neural transplantation (Aubry et al., 2008; Ma et al., 2012; Carri et al., 2013). By contrast, all the 16-week-old grafts in this study were of moderate size, free from proliferation and teratoma/neural overgrowth. Preliminary stereological measurements of the grafts (n=3) revealed average graft volumes of 1.47, 0.78 and 10.66 mm^3 at 4, 8 and 16 weeks, respectively. The number of donor-derived cells per graft at 16 weeks ranged from 2613 to 513,741 cells, with the largest graft comprising 128% of the 400,000 cells transplanted.

DISCUSSION

Derivation of striatal GABAergic neurons from hESCs and hiPSCs presents a powerful platform for understanding human striatal development and a potential alternative cell source for transplantation-based therapy. Moreover, patient iPSCs or hESCs engineered to carry the mutant *HTT* gene with varying CAG repeat lengths create opportunities to understand the pathological cascades that underlie HD and to develop new drugs for this currently incurable neurological disease. However, the HD iPSC models have yet to address the preferential vulnerability of MSNs to the mutant HTT protein due to the relatively low proportion (5%) of $DARPP32^+$ neurons generated using previous Shh-based protocols (The HD iPSC Consortium, 2012). Here we report a novel activity of activin A in the specification of lateral forebrain tissues leading to the reliable generation of $DARPP32^+$ GABAergic neurons. We anticipate that this paradigm can provide a powerful platform for investigations into the specific neurotoxicity of the mutant HTT to striatal MSNs and for developing improved cell-based therapies for HD.

Activin promotes an LGE phenotype

The most pronounced activity of activin in our system was a dramatic and rapid induction of CTIP2, a transcription factor expressed in all developing striatal projection neurons (Arlotta et al., 2008). In a recent study, CTIP2 was reported as the only transcription factor tested that was able to directly reprogram dermal fibroblasts into $DARPP32^+$ neurons, suggesting that it is a potential patterning target of the activin/Smad pathway (Victor et al., 2014). Activin administration also induced the upregulation of other LGE gene markers such as *NOLZ1*, which marks cells leaving the cell cycle in the mantle zone (Chang et al., 2004; Urbán et al., 2010), and *FOXP2*, which marks cells destined for the striosomes (Takahashi et al., 2003). By contrast, activin had little effect on MGE gene markers such as *NKX2.1* and *LHX8*.

The activin-induced gene expression changes are distinct from those induced by Shh, which is the key molecule employed by published striatal differentiation protocols (Aubry et al., 2008; Ma et al., 2012; Nicoleau et al., 2013). These studies and the current work show that Shh elicited a strong inductive effect on MGE regulator genes, such as *NKX2.1*, and gene markers expressed in both the MGE and LGE (e.g. *DLX2* and *GSX2*) in a dose-dependent manner (Sussel et al., 1999; Grigoriou et al., 1998; Flandin et al., 2011). However, little change was observed in the LGE-specific gene expression in response to Shh. Shh is a ventralising morphogen through most of the neural axis (Hébert and Fishell, 2008). In the forebrain, one mechanism by which Shh patterns the subpallium involves antagonising the dorsal signal Gli3 (Rallu et al., 2002). Because the low endogenous levels of SHH signalling are insufficient to trigger ventral gene expression, hESCs have a tendency to acquire a cortical fate by default during differentiation (Li et al., 2009; Espuny-Camacho et al., 2013). Therefore, it would be reasonable to suggest that the main role for Shh in the published striatal differentiation protocols is to suppress dorsal fate rather than to 'direct' a striatal fate.

By contrast, activin is likely to act directly to bias the differentiation fate choice of $FOXG1^+$ forebrain neural progenitors towards an LGE/striatal identity. In addition to the preferential upregulation of LGE-specific or enriched gene markers, EdU incorporation experiments indicate that the activin-induced increase of $GSX2^+$ cells was not due to preferential proliferation of this progenitor population. Rather, the number of EdU^+ cells within the $GSX2^+$ population was reduced in activin-treated cultures compared with controls. This finding is consistent with our previous report that activin treatment reduces the number of cycling forebrain neural progenitors derived from mouse ESCs (Cambray et al., 2012), suggesting a general effect of activin on cell cycle regulation.

Consistent with the lack of $NKX2.1^+$ progenitors, neurons expressing parvalbumin, somatostatin and choline acetyltransferase

Development (2015) 142, 1375-1386 doi:10.1242/dev.117093

(ChAT) were rarely found, providing further evidence that the activin-based differentiation paradigm does not favour MGE fate specification (Miyoshi et al., 2007; Furusho et al., 2006; Goulburn et al., 2012). We showed previously that, when added at a lower concentration and from day 19 of *in vitro* differentiation, activin can induce a CGE neural progenitor identity in hESC-derived forebrain neural progenitors, which subsequently give rise to CR^+ interneurons. CR^+ cells are also observed in the current study in cultures with a higher dose of activin. Interestingly, the temporal timing of activin treatment affects the relative proportion of $DARPP32^+$ and CR^+ neurons. Early (d9) progenitors are potent in generating striatal MSNs, whereas the late progenitors predominantly give rise to CR^+ neurons. This finding is consistent with our past observations that PSC-derived neural progenitors appear to experience a rostral-to-caudal identity shift as *in vitro* differentiation proceeds.

Differentiation and survival of $DARPP32^+$ neurons from activin-induced LGE progenitors following transplantation

PSC-derived neurons in culture are generally immature with regards to electrophysiological properties. This might be due to a lack of maturation stimuli in the environment, including their normal target cell types with which they make synaptic connections. The relatively immature nature of PSC derivatives means that the validation of cellular phenotypes often largely relies on gene marker expression determined by RT-PCR and immunocytochemistry. Cellular transplantation has increasingly been adopted as an additional tool to more fully evaluate the characteristics of defined neuronal subtypes, including the authenticity and functional capacity of hPSC-derived neurons (Espuny-Camacho et al., 2013; Nicholas et al., 2013). Furthermore, for preclinical validation of the potential of these cells it is imperative that they be investigated in animal models of the disease. In this instance the most widely used model of HD, namely the QA lesion rat model, was utilised. Not only does this allow us to look at the maturation of the cells *in vivo* but also provides invaluable information about their propensity to form the appropriate connections required if these cells were to be used for cell replacement therapy strategies. Thus far, we have performed a number of transplants with the activin-induced LGE-like neural progenitors and consistently observed a high proportion of human neurons in grafts derived from activin-induced neural progenitors. Nearly 50% of the graft-derived cells express DARPP32 at 16 weeks post-grafting, as well as other mature MSN molecular markers such as FOXP2 and calbindin, suggesting faithful striatal fate maintenance in the host brains. We also observed some hNCAM-stained neuronal processes extending out from the graft core in an organised fashion (Fig. 6). The location of these graft projections appears to be consistent with the striato-pallido-nigral bundle, where normal MSNs project to the external globus pallidus and to the substantia nigra. However, future studies are required to investigate the extent to which the grafted human neurons can connect to appropriate host brain regions, using techniques such as retrograde labelling and electrophysiological recordings.

Transplantation of hPSC-derived striatal neurons might be developed as a future therapy for HD. To date, a small number of published protocols have reported the differentiation of MSN-like cells *in vitro* and post-transplantation in the rodent brain (Aubry et al., 2008; Ma et al., 2012; Carri et al., 2013). However, evidence is still limited as to the capacity of these cells to integrate into the host neural circuitry and receive dopaminergic inputs from the midbrain and glutamatergic inputs from the cortex while projecting fibres to the substantia nigra. Despite a relatively high content of $DARPP32^+$ cells in our grafts, the recipient animals did not show a difference in apomorphine-induced rotations compared with the pre-grafting baseline. This is intriguing, because we observed a hint of functional recovery in the Carri study (Carri et al., 2013) despite significantly lower numbers of $DARPP32^+$ cells (the number of animals was too small to suggest a significant behavioural effect). Activin-treated cell-derived grafts were generally low in mass compared with those reported in the Ma and Carri studies (Ma et al., 2012; Carri et al., 2013), which might impact on the behavioural analysis. Furthermore, it should be noted that there is no evidence as yet from animal studies that primary human fetal cells can produce a functional effect in such tests as drug-induced rotations or other motor tests (e.g. staircase or rotomotor). Therefore, there are no baseline data against which one can compare the effectiveness of these cells, other than that achieved in allograft experiments of rodent tissues. For the future development of these studies it is important that we identify behavioural tests that will accurately reflect the effect that these cells might have upon integration into the rodent brain.

It is worth noting that the fetal striatal transplantation that led to a positive behavioural effect was achieved with the whole GE, which contains MGE progenitors that give rise to GABAergic interneurons. Therefore, the behavioural recovery reported by Ma et al. (2012) and the hint of improved rotation we observed in Carri et al. (2013) might be attributed, at least in part, to the presence of interneurons induced by Shh.

We observed a substantial delay in DARPP32 expression in the graft compared with sister cultures *in vitro*. This might be attributed to the different niche that the cells are exposed to in culture versus in the host brains. In culture, continued exposure to activin would promote GABAergic maturation due to its reported pro-differentiation activity (Cambray et al., 2012). The neurotrophic factors (BDNF, GDNF) that are added to the cultures might not be experienced by transplanted cells in the host brain. At the time of transplantation, cultures were a mixture of dividing neural progenitors and immature postmitotic neurons. Previous dopaminergic transplantation studies demonstrated that postmitotic neurons do not survive as well as progenitor cells. Therefore, it is possible that young neurons died during and/or soon after transplantation and those $DARPP32^+$ neurons found in the graft are mostly generated from the surviving progenitors. Lastly, *in vitro*, cells were cultured as monolayer with frequent changes of medium and hence might be exposed to lower levels of paracrine proliferative signals than grafted cells in the host striatum.

In conclusion, we demonstrate here that activin signalling is able to promote the differentiation of MSNs *in vitro*, which, upon transplantation into the HD rodent brain, can survive and further differentiate into mature MSNs without any evidence of overgrowth or tumour formation. We can infer a similar role in the developing embryo and this is reinforced by evidence of SMAD2 signalling in the developing basal ganglia. We also present a novel method for producing MSNs *in vitro* that might prove useful for further work on this cell type, including drug screening and cell replacement regimes.

MATERIALS AND METHODS

Cell culture

hESCs (lines H1, H7) and hiPSCs (lines 2F8, 4FH) were maintained, for the majority of this study, on feeder cells in knockout DMEM supplemented with 24% knockout serum replacement (KSR; Life

Development (2015) 142, 1375-1386 doi:10.1242/dev.117093

Technologies) and 8 ng/ml bFGF (FGF2; PeproTech). Some experiments, and all experiments on H9 cells, were performed using hPSCs maintained under our current routine: feeder-free in TeSRTM1 (Stemcell Technologies). All lines were passaged via manual dissociation using 0.02% EDTA pH 7.2. For differentiation, hPSCs were preplated on gelatin for 45 min to remove feeder cells and then plated on Matrigel in feeder conditioned media. Feeder-free cultured hPSCs were plated directly on Matrigel in TeSRTM1. When cells reached >80% confluence in feeder conditioned media or mTeSRTM1, differentiation was then initiated by switching to DMEM-F12/Neurobasal media (2:1) supplemented with N2 (Life Technologies) and retinol-free B27 (Life Technologies) (together referred to as N2B27).

For the first 10 days, cultures were supplemented with SB431542 (10 µM; Tocris), LDN-193189 (100 nM; StemGene) and dorsomorphin (200 nM; Tocris). Some initial experiments were performed with noggin (100 ng/ml; R&D) instead of LDN. Where indicated, Shh (200 ng/ml; recombinant human, C24II-N, R&D) or cyclopamine (2 µM; Sigma) was added to the cultures. Splitting was performed *en bloc* using EDTA either once onto poly-D-lysine/laminin or twice (H7 cells) onto fibronectin and then poly-D-lysine/laminin. Cells remained in basal N2B27 or were supplemented with activin A (25 ng/ml; R&D) from day 9. BDNF, GDNF (10 ng/ml each; Peprotech) were added from day 28 to aid neuronal maturation and survival.

For the proliferation assay, EdU was added to the culture medium for 1 h and then visualised as per the manufacturer's instructions (Life Technologies). Normal B27 was used from day 20 onwards.

Immunocytochemistry

Antibody staining was performed as described (Cambray et al., 2012). Further information, including details of the antibodies used, is provided in the supplementary Materials and Methods.

Quantitative PCR (qPCR)

Marker expression was assessed by qPCR as described in the supplementary Materials and Methods and Table S2.

Electrophysiology

H7 hESCs were differentiated following the scheme illustrated in Fig. 3A, but with the maintenance extended for up to 93 days. Whole-cell electrophysiological recordings were performed and analysed as detailed in the supplementary Materials and Methods.

Transplantation

Transplantation surgeries were performed as reported previously (Kelly et al., 2007, 2011) and are described in detail in the supplementary Materials and Methods. All animal experiments were performed in full compliance with the UK Animals (Scientific Procedures) Act 1986 and approved by local ethical review.

Statistics

SPSS software (IBM) was used for statistical analysis. Comparison of mean values was conducted with paired and/or unpaired Student's *t*-test, one-way ANOVA, two-way ANOVA or repeat measures of general linear model (GLM) analysis. In all analyses, data were obtained from culture experiments comprising at least three biological replica cultures. Data are expressed as mean±s.e.m. and differences were considered statistically significant at $P<0.05$.

Acknowledgements

We thank Drs Austin Smith and Yasuhiro Takashima for providing 2F8 and Kuo Hsuan Chang for the 4FH hiPSC lines.

Competing interests

The authors declare no competing or financial interests.

Author contributions

C.A., S.C., T.A.R. and M.L. conceived and designed the study. C.A., Z.N. and M.F. carried out and analysed the hPSC experiments and C.A. the immunohistochemical analysis of the grafts. J.R.R.-J. and M.A.U. performed and analysed the electrophysiological studies. S.V.P., C.K., A.H., A.E.R. and S.B.D. designed and performed the transplantation. C.A. and M.L. wrote the paper. All authors edited the paper.

Funding

This work was supported by funding from the UK Medical Research Council to M.L., T.A.R., M.A.U., A.E.R. and S.B.D.; EU Framework Programme 7 Neurostemcell and Repair-HD to M.L., A.E.R. and S.B.D.; and a Royal Society University Research Fellowship to M.A.U. Deposited in PMC for release after 6 months.

Supplementary material

Supplementary material available online at
http://dev.biologists.org/lookup/suppl/doi:10.1242/dev.117093/-/DC1

References

Abdipranoto-Cowley, A., Park, J. S., Croucher, D., Daniel, J., Henshall, S., Galbraith, S., Mervin, K. and Vissel, B. (2009). Activin A is essential for neurogenesis following neurodegeneration. *Stem Cells* **27**, 1330-1346.

Arlotta, P., Molyneaux, B. J., Jabaudon, D., Yoshida, Y. and Macklis, J. D. (2008). Ctip2 controls the differentiation of medium spiny neurons and the establishment of the cellular architecture of the striatum. *J. Neurosci.* **28**, 622-632.

Aubry, L., Bugi, A., Lefort, N., Rousseau, F., Peschanski, M. and Perrier, A. L. (2008). Striatal progenitors derived from human ES cells mature into DARPP32 neurons in vitro and in quinolinic acid-lesioned rats. *Proc. Natl. Acad. Sci. USA* **105**, 16707-16712.

Backman, M., Machon, O., Mygland, L., van den Bout, C. J., Zhong, W., Taketo, M. M. and Krauss, S. (2005). Effects of canonical Wnt signaling on dorso-ventral specification of the mouse telencephalon. *Dev. Biol.* **279**, 155-168.

Cambray, S., Arber, C., Little, G., Dougalis, A. G., de Paola, V., Ungless, M. A., Li, M. and Rodríguez, T. A. (2012). Activin induces cortical interneuron identity and differentiation in embryonic stem cell-derived telencephalic neural precursors. *Nat. Commun.* **3**, 841.

Campbell, K. (2003). Dorsal-ventral patterning in the mammalian telencephalon. *Curr. Opin. Neurobiol.* **13**, 50-56.

Carri, A. D., Onorati, M., Lelos, M. J., Castiglioni, V., Faedo, A., Menon, R., Camnasio, S., Vuono, R., Spaiardi, P., Talpo, F. et al. (2013). Developmentally coordinated extrinsic signals drive human pluripotent stem cell differentiation toward authentic DARPP-32+ medium-sized spiny neurons. *Development* **140**, 301-312.

Chang, C.-W., Tsai, C.-W., Wang, H.-F., Tsai, H.-C., Chen, H.-Y., Tsai, T.-F., Takahashi, H., Li, H.-Y., Fann, M.-J., Yang, C.-W. et al. (2004). Identification of a developmentally regulated striatum-enriched zinc-finger gene, Nolz-1, in the mammalian brain. *Proc. Natl. Acad. Sci. USA* **101**, 2613-2618.

Chen, X., Grisham, W. and Arnold, A. P. (2009). X chromosome number causes sex differences in gene expression in adult mouse striatum. *Eur. J. Neurosci.* **29**, 768-776.

Elkabetz, Y., Panagiotakos, G., Al Shamy, G., Socci, N. D., Tabar, V. and Studer, L. (2008). Human ES cell-derived neural rosettes reveal a functionally distinct early neural stem cell stage. *Genes Dev.* **22**, 152-165.

Espuny-Camacho, I., Michelsen, K. A., Gall, D., Linaro, D., Hasche, A., Bonnefont, J., Bali, C., Orduz, D., Bilheu, A., Herpoel, A. et al. (2013). Pyramidal neurons derived from human pluripotent stem cells integrate efficiently into mouse brain circuits in vivo. *Neuron* **77**, 440-456.

Feijen, A., Goumans, M. J. and van den Eijnden-van Raaij, A. J. (1994). Expression of activin subunits, activin receptors and follistatin in postimplantation mouse embryos suggests specific developmental functions for different activins. *Development* **120**, 3621-3637.

Flames, N., Pla, R., Gelman, D. M., Rubenstein, J. L. R., Puelles, L. and Marin, O. (2007). Delineation of multiple subpallial progenitor domains by the combinatorial expression of transcriptional codes. *J. Neurosci.* **27**, 9682-9695.

Flandin, P., Zhao, Y., Vogt, D., Jeong, J., Long, J., Potter, G., Westphal, H. and Rubenstein, J. L. R. (2011). Lhx6 and Lhx8 coordinately induce neuronal expression of Shh that controls the generation of interneuron progenitors. *Neuron* **70**, 939-950.

Furusho, M., Ono, K., Takebayashi, H., Masahira, N., Kagawa, T., Ikeda, K. and Ikenaka, K. (2006). Involvement of the Olig2 transcription factor in cholinergic neuron development of the basal forebrain. *Dev. Biol.* **293**, 348-357.

Garel, S., Marin, F., Grosschedl, R. and Charnay, P. (1999). Ebf1 controls early cell differentiation in the embryonic striatum. *Development* **126**, 5285-5294.

Gennet, N., Gale, E., Nan, X., Farley, E., Takacs, K., Oberwallner, B., Chambers, D. and Li, M. (2011). Doublesex and mab-3-related transcription factor 5 promotes midbrain dopaminergic identity in pluripotent stem cells by enforcing a ventral-medial progenitor fate. *Proc. Natl. Acad. Sci. USA* **108**, 9131-9136.

Gerfen, C. R. (1992). The neostriatal mosaic: multiple levels of compartmental organization in the basal ganglia. *Annu. Rev. Neurosci.* **15**, 285-320.

Development (2015) 142, 1375-1386 doi:10.1242/dev.117093

Goulburn, A. L., Stanley, E. G., Elefanty, A. G. and Anderson, S. A. (2012). Generating GABAergic cerebral cortical interneurons from mouse and human embryonic stem cells. *Stem Cell Res.* **8**, 416-426.

Grigoriou, M., Tucker, A. S., Sharpe, P. T. and Pachnis, V. (1998). Expression and regulation of Lhx6 and Lhx7, a novel subfamily of LIM homeodomain encoding genes, suggests a role in mammalian head development. *Development* **125**, 2063-2074.

Gulacsi, A. and Anderson, S. A. (2006). Shh maintains Nkx2.1 in the MGE by a Gli3-independent mechanism. *Cereb. Cortex* **16** Suppl. 1, i89-i95.

Harrison-Uy, S. J. and Pleasure, S. J. (2012). Wnt signaling and forebrain development. *Cold Spring Harb. Perspect. Biol.* **4**, a008094.

Hébert, J. M. and Fishell, G. (2008). The genetics of early telencephalon patterning: some assembly required. *Nat. Rev. Neurosci.* **9**, 678-685.

Kelly, C. M., Precious, S. V., Penketh, R., Amso, N., Dunnett, S. B. and Rosser, A. E. (2007). Striatal graft projections are influenced by donor cell type and not the immunogenic background. *Brain* **130**, 1317-1329.

Kelly, C. M., Precious, S. V., Torres, E. M., Harrison, A. W., Williams, D., Scherf, C., Weyrauch, U. M., Lane, E. L., Allen, N. D., Penketh, R. et al. (2011). Medical terminations of pregnancy: a viable source of tissue for cell replacement therapy for neurodegenerative disorders. *Cell Transplant.* **20**, 503-513.

Klapstein, G. J., Fisher, R. S., Zanjani, H., Cepeda, C., Jokel, E. S., Chesselet, M. F. and Levine, M. S. (2001). Electrophysiological and morphological changes in striatal spiny neurons in R6/2 Huntington's disease transgenic mice. *J. Neurophysiol.* **86**, 2667-2677.

Lange, H., Thörner, G., Hopf, A. and Schröder, K. F. (1976). Morphometric studies of the neuropathological changes in choreatic diseases. *J. Neurol. Sci.* **28**, 401-425.

Li, X.-J., Zhang, X., Johnson, M. A., Wang, Z.-B., LaVaute, T. and Zhang, S.-C. (2009). Coordination of sonic hedgehog and Wnt signaling determines ventral and dorsal telencephalic neuron types from human embryonic stem cells. *Development* **136**, 4055-4063.

Ma, L., Hu, B., Liu, Y., Vermilyea, S. C., Liu, H., Gao, L., Sun, Y., Zhang, X. and Zhang, S.-C. (2012). Human embryonic stem cell-derived GABA neurons correct locomotion deficits in quinolinic acid-lesioned mice. *Cell Stem Cell* **10**, 455-464.

Machold, R., Hayashi, S., Rutlin, M., Muzumdar, M. D., Nery, S., Corbin, J. G., Gritli-Linde, A., Dellovade, T., Porter, J. A., Rubin, L. L. et al. (2003). Sonic hedgehog is required for progenitor cell maintenance in telencephalic stem cell niches. *Neuron* **39**, 937-950.

Magnani, D., Hasenpusch-Theil, K., Jacobs, E. C., Campagnoni, A. T., Price, D. J. and Theil, T. (2010). The Gli3 hypomorphic mutation Pdn causes selective impairment in the growth, patterning, and axon guidance capability of the lateral ganglionic eminence. *J. Neurosci.* **30**, 13883-13894.

Maira, M., Long, J. E., Lee, A. Y., Rubenstein, J. L. R. and Stifani, S. (2010). Role for TGF-beta superfamily signaling in telencephalic GABAergic neuron development. *J. Neurodev. Disord.* **2**, 48-60.

Manning, L., Ohyama, K., Saeger, B., Hatano, O., Wilson, S. A., Logan, M. and Placzek, M. (2006). Regional morphogenesis in the hypothalamus: a BMP-Tbx2 pathway coordinates fate and proliferation through Shh downregulation. *Dev. Cell* **11**, 873-885.

Marín, O. and Rubenstein, J. L. R. (2003). Cell migration in the forebrain. *Annu. Rev. Neurosci.* **26**, 441-483.

Miyoshi, G., Butt, S. J. B., Takebayashi, H. and Fishell, G. (2007). Physiologically distinct temporal cohorts of cortical interneurons arise from telencephalic olig2-expressing precursors. *J. Neurosci.* **27**, 7786-7798.

Nicholas, C. R., Chen, J., Tang, Y., Southwell, D. G., Chalmers, N., Vogt, D., Arnold, C. M., Chen, Y.-J. J., Stanley, E. G., Elefanty, A. G. et al. (2013). Functional maturation of hPSC-derived forebrain interneurons requires an extended timeline and mimics human neural development. *Cell Stem Cell* **12**, 573-586.

Nicoleau, C., Varela, C., Bonnefond, C., Maury, Y., Bugi, A., Aubry, L., Viegas, P., Bourgois-Rocha, F., Peschanski, M. and Perrier, A. L. (2013). Embryonic stem cells neural differentiation qualifies the role of Wnt/beta-Catenin signals in human telencephalic specification and regionalization. *Stem Cells* **31**, 1763-1774.

Nikoletopoulou, V., Plachta, N., Allen, N. D., Pinto, L., Götz, M. and Barde, Y.-A. (2007). Neurotrophin receptor-mediated death of misspecified neurons generated from embryonic stem cells lacking pax6. *Cell Stem Cell* **1**, 529-540.

Nisenbaum, E. S., Xu, Z. C. and Wilson, C. J. (1994). Contribution of a slowly inactivating potassium current to the transition to firing of neostriatal spiny projection neurons. *J. Neurophysiol.* **71**, 1174-1189.

Olsson, M., Björklund, A. and Campbell, K. (1998). Early specification of striatal projection neurons and interneuronal subtypes in the lateral and medial ganglionic eminence. *Neuroscience* **84**, 867-876.

Ouimet, C. C., Miller, P. E., Hemmings, H. C., Jr, Walaas, S. I. and Greengard, P. (1984). DARPP-32, a dopamine- and adenosine 3′:5′-monophosphate-regulated phosphoprotein enriched in dopamine-innervated brain regions. III. Immunocytochemical localization. *J. Neurosci.* **4**, 111-124.

Rallu, M., Machold, R., Gaiano, N., Corbin, J. G., McMahon, A. P. and Fishell, G. (2002). Dorsoventral patterning is established in the telencephalon of mutants lacking both Gli3 and hedgehog signaling. *Development* **129**, 4963-4974.

Reiner, A., Albin, R. L., Anderson, K. D., D'Amato, C. J., Penney, J. B. and Young, A. B. (1988). Differential loss of striatal projection neurons in Huntington disease. *Proc. Natl. Acad. Sci. USA* **85**, 5733-5737.

Rosser, A. E. and Bachoud-Lévi, A.-C. (2012). Clinical trials of neural transplantation in Huntington's disease. *Prog. Brain Res.* **200**, 345-371.

Sekiguchi, M., Hayashi, F., Tsuchida, K. and Inokuchi, K. (2009). Neuron type-selective effects of activin on development of the hippocampus. *Neurosci. Lett.* **452**, 232-237.

Sussel, L., Marin, O., Kimura, S. and Rubenstein, J. L. R. (1999). Loss of Nkx2.1 homeobox gene function results in a ventral to dorsal molecular respecification within the basal telencephalon: evidence for a transformation of the pallidum into the striatum. *Development* **126**, 3359-3370.

Takahashi, K., Liu, F.-C., Hirokawa, K. and Takahashi, H. (2003). Expression of Foxp2, a gene involved in speech and language, in the developing and adult striatum. *J. Neurosci. Res.* **73**, 61-72.

The HD iPSC Consortium. (2012). Induced pluripotent stem cells from patients with Huntington's disease show CAG-repeat-expansion-associated phenotypes. *Cell Stem Cell* **11**, 264-278.

Uhl, G. R., Navia, B. and Douglas, J. (1988). Differential expression of preproenkephalin and preprodynorphin mRNAs in striatal neurons: high levels of preproenkephalin expression depend on cerebral cortical afferents. *J. Neurosci.* **8**, 4755-4764.

Urbán, N. Martín-Ibáñez, R., Herranz, C., Esgleas, M., Crespo, E., Pardo, M., Crespo-Enríquez, I., Méndez-Gómez, H. R., Waclaw, R., Chatzi, C. et al. (2010). Nolz1 promotes striatal neurogenesis through the regulation of retinoic acid signaling. *Neural Dev.* **5**, 21.

Victor, M. B., Richner, M., Hermanstyne, T. O., Ransdell, J. L., Sobieski, C., Deng, P.-Y., Klyachko, V. A., Nerbonne, J. M. and Yoo, A. S. (2014). Generation of human striatal neurons by microRNA-dependent direct conversion of fibroblasts. *Neuron* **84**, 311-323.

Xu, Q., Guo, L., Moore, H., Waclaw, R. R., Campbell, K. and Anderson, S. A. (2010). Sonic hedgehog signaling confers ventral telencephalic progenitors with distinct cortical interneuron fates. *Neuron* **65**, 328-340.

Xuan, S., Baptista, C. A., Balas, G., Tao, W., Soares, V. C. and Lai, E. (1995). Winged helix transcription factor BF-1 is essential for the development of the cerebral hemispheres. *Neuron* **14**, 1141-1152.

Zhao, Y., Marin, O., Hermesz, E., Powell, A., Flames, N., Palkovits, M., Rubenstein, J. L. R. and Westphal, H. (2003). The LIM-homeobox gene Lhx8 is required for the development of many cholinergic neurons in the mouse forebrain. *Proc. Natl. Acad. Sci. USA* **100**, 9005-9010.

Supplementary Materials and Methods

Immunocytochemistry

Cells and brain sections were rinsed in PBS and fixed in 3.7% PFA for 15 min. FOXG1 antibody staining was performed with methanol-acetone fixation. Cells were permeabilised via three washes in PBS containing 0.3% Triton X-100 (PBST) and then blocked in PBST containing 1% BSA and 3% normal donkey serum. Primary antibodies were added in blocking solution for 2 hours at ambient temperature or overnight at 4ºC. The cells were washed in PBST three times before being incubated for 1 hour in the dark in Alexa-Fluor secondary antibodies, 1:200 (Invitrogen). Three PBST washes were then performed that included one with DAPI, 1:1000 (Molecular Probes). The primary antibodies used in this study were: Calbindin (Swant, CB-38a, 1:500), CTIP2 (Abcam, 25B6, 1:500), DARPP32 (Santa Cruz, sc 11365, 1:200), DLX2 (Millipore, ab5726, 1:300), ENK (Immunostar, 20065, 1:400), SubP (Immunostar, 20064, 1:400), Forse1 (DSHB, 1:100), FOXP2 (Abcam, ab58599, 1:100), FOXG1 (Abcam, ab5274,1:250), GABA (Sigma, A2052, 1:500), GAD65/67 (Sigma, G5163, 1:1000), GSX2 (Millipore, abn162, 1:1000), HuNu (Millipore, mab1281, 1:250), hNCAM (Santa Cruz, sc-106, 1:200), MAP2 (Sigma, M1406, 1:250), Nestin (BD, 611659, 1:300), NeuN (Millipore, mab377, 1:250), NKX2.1 (Abcam, ab40880, 1:1000), OTX2 (Millipore, ab9566, 1:300), PAX6 (DSHB, 1:1000), PSD95 (Thermo Scientific, 6G6-1C9, 1:200), TH (Pelfreez, P40101, 1:500). Images were taken on a Leica TCS SP5 confocal microscope. Quantification of markers was carried out manually by examining randomly selected fields from at least three independent experiments and presented as mean ± sem. Statistical significance was determined using two-tailed Student's t-test.

Quantitative PCR

Total RNA was extracted using TRI Reagent (Sigma) according to the manufacturer's instructions. Reverse transcription was performed using SS RTIII (Invitrogen). qPCR was carried out using SYBR MESA Green and a Chromo4 machine (BioRad). All data are relative to three reference genes (*GAPDH, b-ACTIN, CYCLOPHILIN*) and normalised to the basal conditions. The sequence information for all PCR primers can be found in Table S2. All qPCR data are presented as mean ± s.e.m. of biological duplicates or triplicates.

Electrophysiology

H7 hESCs were differentiated following the scheme illustrated in Fig. 3A but the maintenance was extended for up to 93 days. On the day of recording, neurons were placed on a recording chamber and viewed using an Olympus BX51WI microscope with a 40x water immersion lens and DIC (differential interference contrast) optics. Cells were bathed in a solution containing (in mM): 140 NaCl, 3.5 KCl, 1.25 NaH_2PO_4, 2 $CaCl_2$, 1 $MgCl_2$, 10 glucose, and 10 HEPES. For whole-cell electrophysiological recordings, low resistance recording pipettes (10-15 MΩ) were pulled from capillary glass (Harvard Apparatus) and coated with ski wax to reduce pipette capacitance. Recording pipettes were filled with a solution containing (in mM): 140 K-gluconate, 5 NaCl, 2 Mg-ATP, 0.5 LiGTP, 0.1 $CaCl_2$, 1 $MgCl_2$, 1 ethylene glycol-bis (b-aminoethyl ether) -N,N,N,N-tetraacetic acid (EGTA), and 10 HEPES. Osmolarity and pH of both solutions were adjusted before recordings. For mIPSCs, pipettes were filled with a high-chloride solution containing (in mM): 135 CsCl, 4 NaCl, 2 ATP, 0.3 GTP, 0.5 $MgCl_2$, 2 EGTA, and 10 HEPES. TTX (1 µM) was added to the external solution. Data were acquired at room temperature using an Axon Multiclamp 700B amplifier and a Digidata 1440a acquisition system, with pClamp 10 software (Molecular Devices). Data analysis was carried out using Clampfit 10.2 software (Axon Instruments), OriginPro 8.1 (OriginLab Corporation), and Spike2v5 software (Cambridge Electronic Design).

Transplantation

All animal experiments were performed in full compliance with the UK Animals (Scientific Procedures) Act 1986 and approved by local ethical review. Adult female Sprague-Dawley rats (Harlan, UK) weighing 200-250 g at the start of the experiment were used. Rats received unilateral injections of 45 nmol quinolinic acid to the right striatum, at stereotaxic coordinates: +0.4/+1.4 mm anterior (A) of bregma, -3.2/-2.4 mm lateral (L) of bregma, and -5.0/-4.5 mm below dura, as described previously (Kelly et al., 2007). Rats received unilateral transplants of activin-treated H7 hESC-derived neural progenitors harvested at day 20. $4x10^5$ cells were injected in a final volume of 2 µl into the lesioned striatum at stereotaxic coordinates, from bregma: +0.8 mm A, -2.8 mm L and -5.0/-4.5 mm below dura. Transplanted adult rats received immunosuppression in the form of daily cyclosporin A (CsA, Sandimmun, 10 mg/kg, i.p.) commencing the day prior to transplantation and continuing for the

duration of the experiment. Rats were sacrificed at 4, 8 and 16 weeks post transplantation, by barbiturate overdose and transcardial perfusion, as described previously (Kelly et al., 2011). Brains were sectioned coronally at 40 µm, collected in Tris-buffer with azide and were processed for immunohistochemistry.

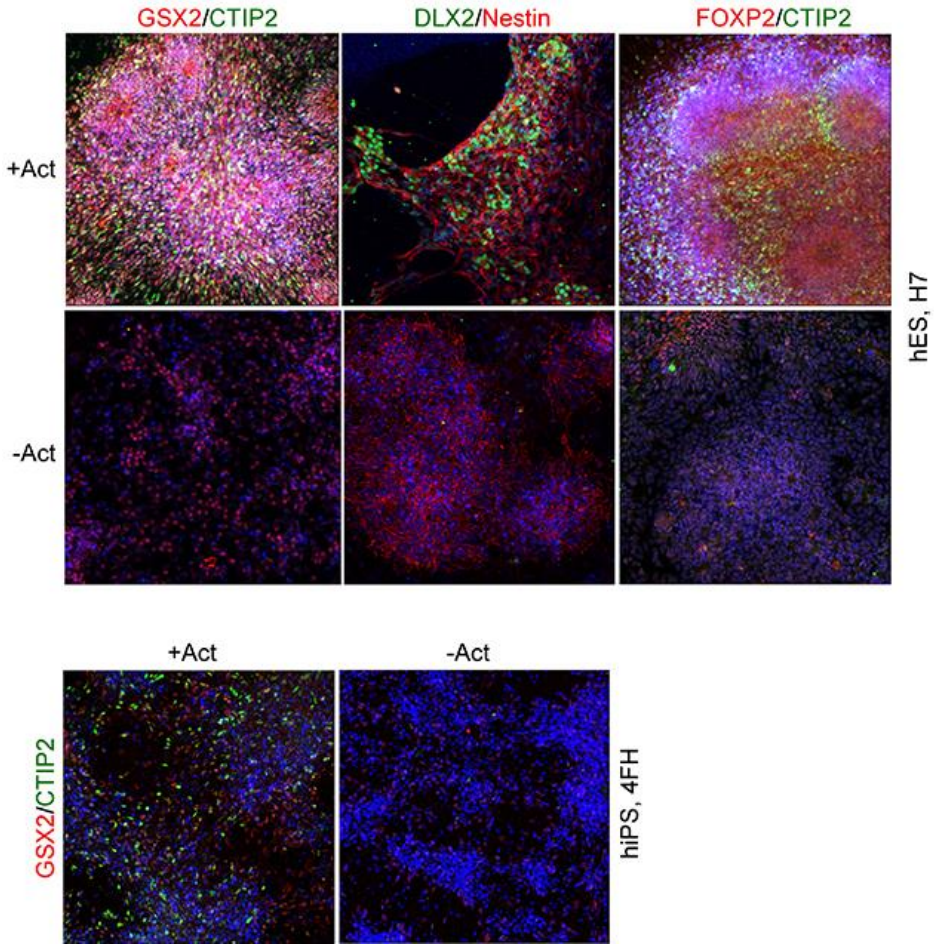

Fig. S1. Activin induces LGE progenitor characteristics and striatal differentiation of hPSCs.

The same as Fig. 1G with DAPI counterstain in blue. Day 22 cultures of H7 hESCs and day 18 cultures of 4FH hiPSCs exposed to activin from day 9 were double immunostained for GSX2 and CTIP2; DLX2 and Nestin; and FOXP2 and CTIP2.

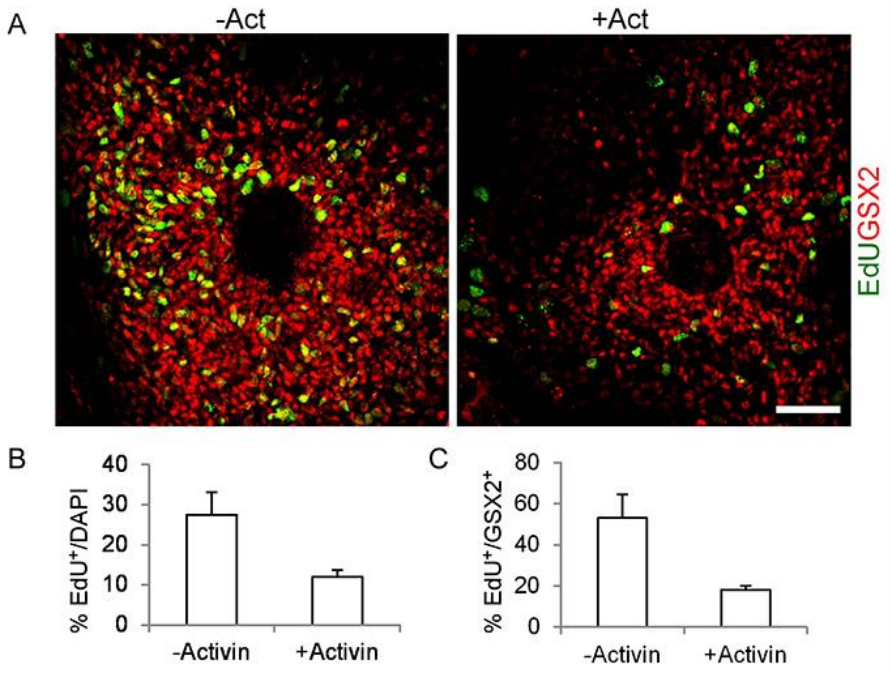

Fig.S2. Activin does not induce preferential proliferation of GSX2$^+$ progenitor characteristics.

A, Chemical and immunostaining of day16 cultures for EdU and GSX2, respectively.

B-C, Quantification of the above illustrating the percentage of cells expressing EdU.

Scale bar: 50 μm.

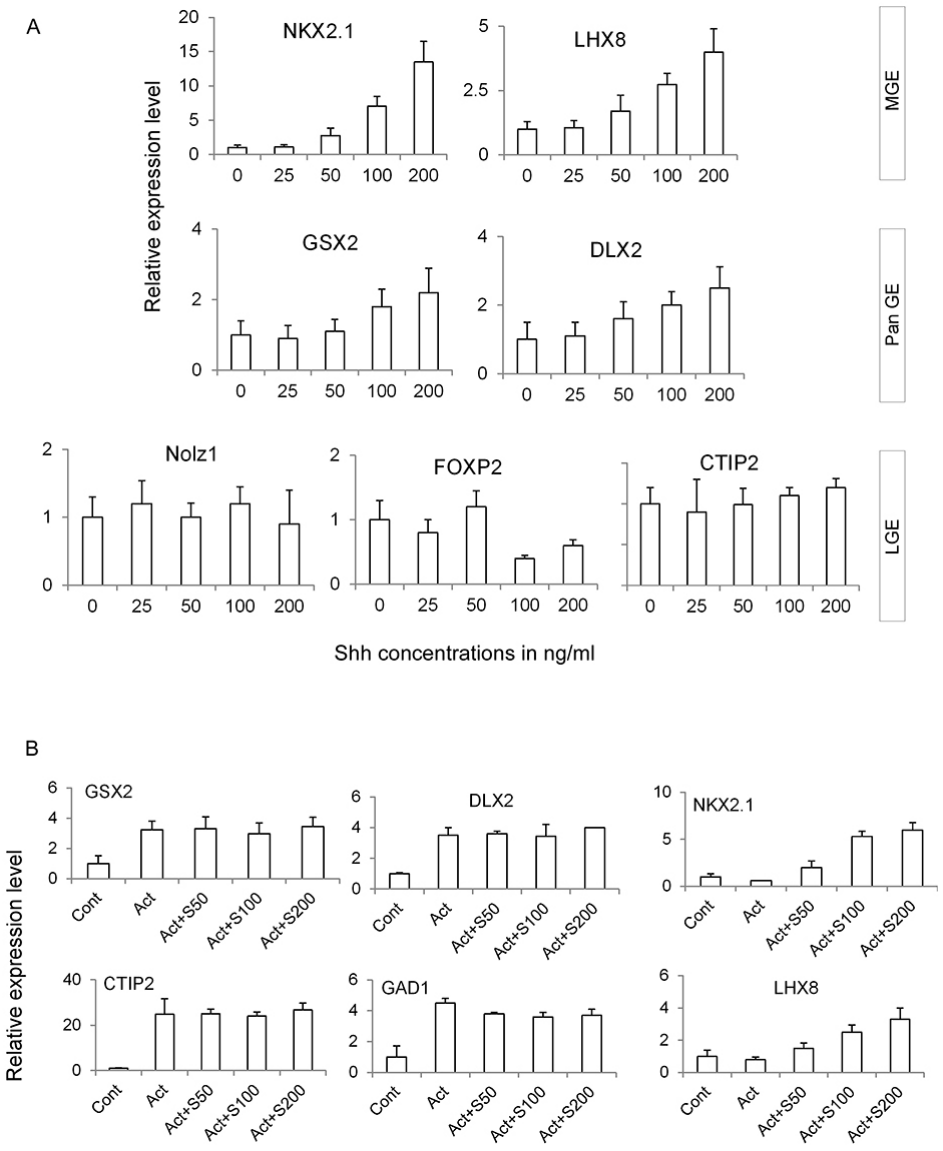

Fig. S3. Activin-induced striatal fate does not involve SHH signalling.

A, Day 9 cultures were treated with increasing concentrations of SHH for 4 days. Cultures were then processed for qPCR analysis to examine the effect of SHH on MGE and LGE expressed genes.

B, Day 9 cultures were treated with activin (Act) with or without increasing concentrations of SHH. Cultures were harvested 4 days later for qPCR.

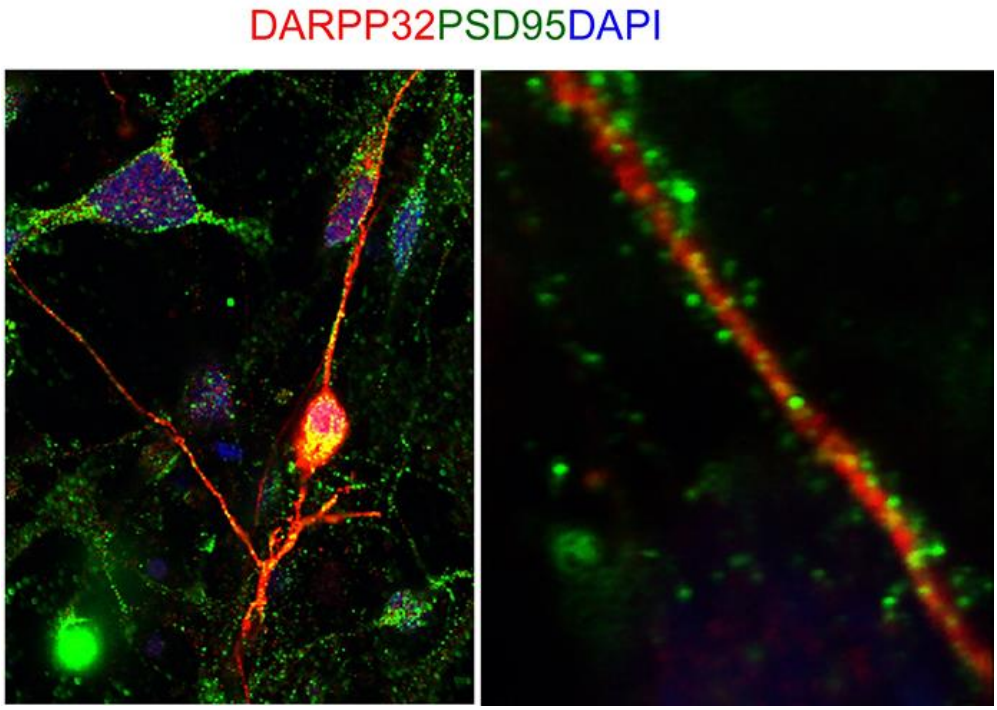

Fig. S4. Expression of post-synaptic protein PSD95 by hESC-derived striatal neurons.

Day 35 cultures treated with activin from day 9 were double stained for DARPP32 and PSD95. The right panel shows accumulation of PSD95 on spines and dendrites of DARPP32^{+} neurons.

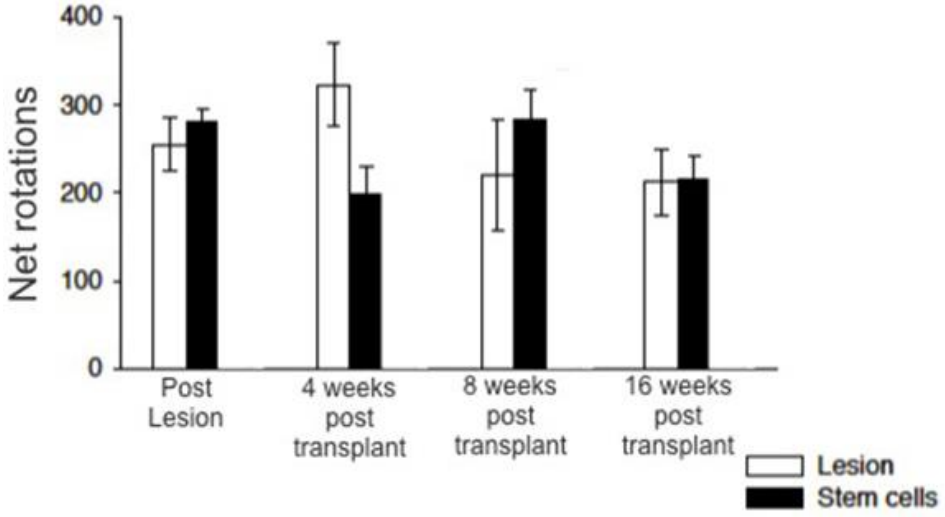

Fig. S5. Functional assessment of the hESC grafts transplantation into rat striatum.

Apomorphine-induced rotations rotation test at 4, 8 and 16 weeks after transplantation. No improvement was observed.

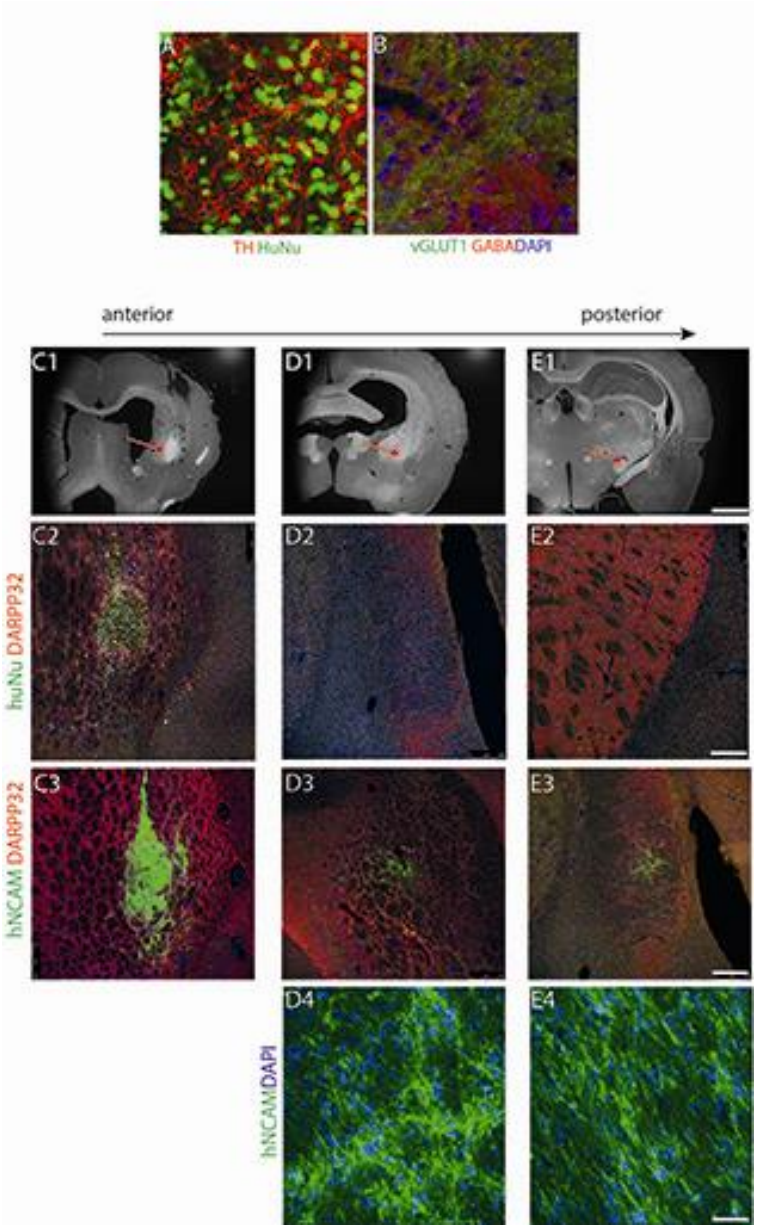

Fig S6. Analysis of graft cell integration in the host brain.

A-B, a section crossing the centre of a 16 week old graft double stained for TH and HuNu in (A), and vGLUT1 and GABA with DAPI counter stain in (B). C. Shown are coronal sections of rat brains 16 weeks post-transplant through the forebrain and striatum (C1-4), globus pallidus (D1-4) and the substantia nigra in the midbrain (E1-4). Arrows mark the location of the high power images below. Immunostaining for DARPP32, HuNu and hNCAM reveal human nuclei in the striatum (graft location,C2) and hNCAM projecting caudally towards the globus pallidus (D3-4) and midbrain (E3-4). Scale bars: 3mm for C1, D1, E1; 400μm for C2-3, D2-3 and E2-3; 60 μm for D4 and E4.

Table S1. Electrophysiological properties of neurons during differentiation

Group:	**d30-49**	**d50-69**	**>d70**	**ALL**
N=	12	21	8	41
Resting Membrane Potential (mV)	-41.2 ± 3.57	-44.8 ± 2.36	-47.7 ± 2.98	-44.3 ± 1.7
N=	17	28	15	60
Capacitance (pF)	20 ± 1.94	22.4 ± 2.02	29.3 ± 3.95	23.7 ± 1.54
Input Resistance (mW)	686 ± 66.9	942 ± 255	502 ± 81.4	760 ± 123
N=	17	28	13	58
Series Resistance (mW)	15.6 ± 1.56	16.1 ± 1.22	16.6 ± 1.29	16.0 ± 0.79

Table S2. PCR primers

ARPP21	GGAAGCTGGTTGACGATGTGTC	GGCTTCTGTCGTTCTACGCC
βActin	TCACCACCACGGCCGAGCG	TCTCCTTCTGCATCCTGTCG
Calbindin	ATCAGGACGGCAATGGATAC	TAAGAGCAAGATCCGTTCGG
CTIP2	CTCCGAGCTCAGGAAAGTGTC	TCATCTTTACCTGCAATGTTCTCC
Cyclophilin	GGCAAATGCTGGACCAAACAC	TTCCTGGACCCAAAACGCTC
DARPP32	TTGGAAAATCCAGAAAACCG	CTGGTAGAAGCCGGTGAGAG
DLX2	ACTACCCCTGGTACCACCAGAC	TCTGCTCTCAGTCTCTGGCGAGTTCTC
DRD2	CTGAGGGCTCCACTAAAGGAG	CATTCTTCTCTGGTTTGGCG
EBF1	AATGTAAGCAAGGTGGACGC	TCAAGGTCTAAGCCGGACAC
FOXP2	AATGTGGGAGCCATACGAAG	GCCTGCCTTATGAGAGTTGC
GAD67	CGTCTTCGACCCCATCTTCGT	CGCAGATCTTGAGCCCCAGTT
GAPDH	ATGACATCAAGAAGGTGGTG	CATACCAGGAAATGAGCTTG
GLI1	TGAGGCCCTTCAAAGCCC	GTATGACTTCCGGCACCCTTC
GSX2	TCACTAGCACGCAACTCCTG	TTTTCACCTGCTTCTCCGAC
NKX2.1	CGCATCCAATCTCAAGGAAT	TGTGCCCAGAGTGAAGTTTG
NOLZ1	ACATTTTGCACCCCGAGTAC	GGAGTACGGCTTGAAACTCG
PAX6	AACAGACACAGCCCTCACAAACA	CGGGAACTTGAACTGGAACTGAC
PENK	GCTGTCCAAACCAGAGCTTC	TCTGGCTCCATGGGATAAAG
PTCH1	TTCGCTCTGGAGCAGATTTCCAAG	GCTTTTAATCCCACCGCGAAG
TAC1	TGGGGTTGAAAATTCAAAAAG	GGAGTTTCCTTCCTTTTCCG
TH	GAGTACACCGCCGAGGAGATTG	GCGGATATACTGGGTGCACTGG
vGLUT1	AGTTCGCAACGATGATGGCA	CTGCACCCCAGCATCTCTGA